SIAM J. CONTROL OPTIM.
Vol. 56, No. 3, pp. 1640–1664

STABILITY ANALYSIS OF POWER SYSTEMS: A NETWORK SYNCHRONIZATION PERSPECTIVE*

LIJUN ZHU† AND DAVID J. HILL†

Abstract. A power network is a large-scale and highly nonlinear dynamical complex system with generators and loads interconnected in a network structure. The transient stability of the power system that we study here refers to its ability for bus angles to remain in synchronism. The usual view of a stable power system is in terms of being able to return from the postfault state to a system equilibrium after severe failures or faults occur. In fact, power systems experience instantaneous load and generation fluctuations even in the absence of system faults. This paper reframes the stability definition in terms of continuous synchronous behavior and looks at the stability of power systems as the capability of withstanding these various fluctuations as external disturbances. The new stability definition is characterized by the property that angles stay cohesive with each other and frequencies of generators stay bounded. The main objective is to establish a stability analysis method based on a class of new energy functions. An important stability lemma is proposed for nonlinear systems which later is used to derive the phase cohesiveness and frequency boundedness conditions. Motivated by the recent study of complex networks, coupled phase oscillators, and synchronization of power systems, the paper also derives a purely algebraic condition showing explicitly how the stability of the power network is related to the underlying network topology, system parameters and affected by the disturbances.

Key words. synchronization, stability analysis, power systems, Lyapunov function

AMS subject classifications. 34D06, 37C75, 93C10, 93D05

DOI. 10.1137/17M1118646

1. Introduction.

A power system is an engineered complex network with heterogeneous nodes representing load and generator buses coupled via electric connections which constitute a network topology. The transient stability of power systems has been long recognized as an important issue for stable and secure system operation in order to deliver electric power reliably from generators to loads. It refers to the system's ability to withstand the occurrence of faults such as short circuits in transmission lines and fluctuations in load demands and characterizes the capability of a postfault trajectory to return to a system equilibrium. Traditional stability assessment approaches are categorized into direct time-domain simulation and energy function methods. Time-domain simulation is straightforward and assesses the stability with respect to a given disturbance by means of numerical integration [21, 29]. Although the accuracy can be guaranteed provided there are correct modeling and precise knowledge of system parameters, time-domain simulation provides less intuitive results and requires intensive computation especially for large-scale power systems. On the contrary, the energy function method determines the system stability using a class of energy functions whose value locally decreases along the system trajectory towards the system equilibrium. The basic method compares the postfault energy with energy at the critical unstable equilibrium point (UEP) [16] such as closest UEP or controlling UEP [7, 8] to conclude the stability result. Since energy function methods

*Received by the editors February 27, 2017; accepted for publication (in revised form) January 19, 2018; published electronically May 8, 2018.
http://www.siam.org/journals/sicon/56-3/M111864.html
Funding: This work was supported by The University of Hong Kong Research Committee Post-doctoral Fellow Scheme.
†Department of Electrical and Electronic Engineering, The University of Hong Kong, Hong Kong (ljzhu@eee.hku.hk, dhill@eee.hku.hk).

adopt Lyapunov stability theory, they provide more insights into the stability problem and are less computing intensive, although the estimated region of attraction is conservative.

A disadvantage of traditional stability assessment approaches, particularly the energy function method, is that real-time disturbances are not accounted for. Over the last decade, the modern power system has seen increasingly large amounts of renewable energy being integrated into grids. The renewable energy has an intermittent and stochastic nature, since the power generated by renewable energy is subjected to weather conditions. Being fed into power grids, it may cause fluctuations in power generation. On the other hand, the power demand within a certain time scale is predicted over time, but the real-time demand is in fact instantaneously fluctuating around the predicted values, especially when new and complicated demand-side activities are stressing the grid. In fact, the ability and tolerance to withstand disturbances and fluctuations generally reflect the robustness of power systems. These issues generate new challenges to the stability of power systems and have yet to be investigated.

The dynamic model of power systems composed of generations and loads is central to the stability analysis. The second-order swing equation is the standard model for the rotor dynamics of conventional generators, while the load model and power network structure are somewhat varied in the literature. The early studies consider the loads in conventional power systems as pure impedances. To facilitate transient stability analysis, a circuit-theoretic method called Kron reduction was adopted to simplify the model [3, 27]. It reduces the original power network into a network merely consisting of generators and, hence, the original network structure is lost. The loads are absorbed as the transfer conductances effectively connecting generators. Even though the original power network is reasonably assumed as lossless, the reduced network cannot be, in general, due to induced transfer conductance. The inclusion of nonzero transfer conductance caused by load absorption has made attempts to develop general Lyapunov functions unsuccessful. Later, Bergen and Hill [4] proposed a frequency-dependent load model and presented the network-preserving model of power systems where Kron reduction was avoided. The advantage of the network-preserving model is to allow the construction of topology-dependent Lyapunov functions as well as Lyapunov functions in Lur'e–Postnikov form [4, 18, 19] for stability analysis. More importantly, the model explicitly preserves the original network topology, making it possible to study the influence of the network topology on the stability. More recently, the trend of the integration of distributed energy sources into the grids, such as wind power, geothermal system, and distributed battery systems, motivates the modeling for these devices. In [1], the model for inverter-based distributed energy sources was first proposed in a network-preserving model of microgrids following the work [4]. A microgrid is a type of low-voltage electrical distribution network consisting of distributed energy sources and loads (see, e.g., [25, 30, 39]). Renewable energies, as the prevailing energy sources in microgrids, are fed via inverters with droop controllers implementing frequency and voltage regulation.

It is recognized that the dynamics of coupled phase oscillators resembles the bus dynamics of power systems [14, 20]. The synchronization phenomena observed in physics and biology [6] led to the celebrated mathematical model for coupled phase oscillators called the Kuramoto model [24, 36]. Potential functions and the LaSalle invariance principle ([22, 28]) were utilized to study the Kuramoto model with uniform natural frequency. For the nonuniform natural frequency case, various necessary [11, 22, 34] and sufficient [11, 12, 13, 17] frequency synchronization conditions were proposed. These results showed that the synchronization condition relies on the coupling strength K satisfying $K > K_c$, where K_c is the critical coupling strength that depends on the local natural frequencies and the number of oscillators. Recently, the second-order Kuramoto model augmented with inertia has been proposed and numerically [32, 33] and theoretically [9, 10] studied for which similar synchronization conditions were discovered. In contrast to power systems, Kuramoto oscillators are assumed to be connected in an all-to-all fashion.

Another inspiring line of work relevant to the stability of power systems is the synchronization of complex networks [5, 26, 31, 35, 37, 38]. Compared with power systems and coupled oscillators, this type of work employs rather simplistic dynamics, linear coupling, and places much more emphasis on the network structure including small-world and scale-free models. Typically, each node in the network has nonlinear dynamics and would locally exhibit rich behaviors such as periodic, quasi-periodic, or chaotic behaviors. When linearly coupled, trajectories of nodes synchronize with each other. The critical coupling strength for the local exponential synchronization is determined by the interplay of local dynamics and the algebraic connectivity of the network [35].

In light of the synchronization of complex networks, it is recognized in [20] that the topological property of the underlining network would have an impact on the transient stability of the power system. In [14], Dörfler and Bullo linked the stability analysis of power system with the synchronization of Kuramoto models. Under the assumption of overdamped generators, the network-reduced model of conventional power grids is approximated into nonuniform Kuramoto oscillators using a singular perturbation argument. An algebraic synchronization condition was derived which related the synchronization to the network topology.

This paper follows the research line of [13, 14, 20] to investigate the transient stability of power systems directly in terms of synchronization. In particular, we will study this problem under persistent external perturbations caused by the fluctuation in power generation and load consumption. To the authors' knowledge, this problem emerges from the recent trends in the high penetration of renewables in grids and it is still an open question. The main contributions of this paper are fourfold. First, we propose a new definition for transient stability analysis in section 3. The phase cohesiveness and frequency boundedness in Definition 2.2 is inspired by [14], but it relaxes exact frequency synchronization in [14] and allows frequencies to be ultimately bounded. This definition enables us to study stability under time-varying perturbation caused by power fluctuation.

Second, we introduce a new coordinate transformation for the analysis instead of using the traditional grounded coordinate as in [4, 19]. Traditional treatment appoints one of the buses as the reference and refers the remaining angles to the reference bus. This results in the so-called grounded model for which one bus is removed from the original network topology. The new coordinate transformation converts the original system into a deviation system that describes how the disturbance drive the angle and frequency to deviate from the equilibrium subspace (which corresponds to the equilibrium point in the grounded model), while the network topology remains explicitly expressed.

Third, we propose a general class of parameterized energy functions for power systems described by the deviation dynamics. By tuning parameters, the parameterized energy function can be used for the stability analysis of different power system models. It is also worth mentioning that the energy function can be reduced to that proposed in [14] and [39] by tuning parameters.

Last but not least, we establish a novel and general stability lemma for nonlinear systems. The energy function and the lemma are both utilized in the stability analysis to derive the synchronization condition for power systems and enable us to explore the stability of the power system without assuming generators are overdamped compared to [14]. As done in [14], we also establish an algebraic condition to connect the synchronization of power systems with the network topology and system parameters.

The rest of the paper is structured as follows. Section 2 introduces the general model for various types of power systems and presents the new stability definition. Section 3 discusses equilibrium points of power systems and introduces a novel coordinate transformation with respect to an equilibrium point and the stability definition is translated into the new coordinates. Section 4 proposes an important stability lemma for nonlinear systems, which is used to derive synchronization conditions under a new stability definition in section 5, where a class of parameterized energy functions is obtained. Followed by section 6, the so-called synchronizability condition is obtained that relates the synchronization with the network topology, system parameters, and also shows how it is affected by the disturbances. Section 7 conducts the small disturbance analysis and section 8 verifies theoretical results on the IEEE 9-bus test system using numerical simulation. The paper is concluded in section 9.

Notations. For a vector $x \in \mathbb{R}^n$, $\|x\|$ and $\|x\|_\infty$ are the 2-norm and ∞-norm of vector x and $\sin(x) := [\sin(x_1), \ldots, \sin(x_n)]^{\mathrm{T}}$. For a scalar x, the function $\mathrm{sinc}(x)$ is defined as $\mathrm{sinc}(x) = \sin x/x$. Vectors e_n and 0_n are column vectors of dimension n with all elements being 1 and 0, respectively. For instance, $e_q = [1, \ldots, 1]^{\mathrm{T}} \in \mathbb{R}^q$. Let $O_{n\times m}$ be the zero matrix of dimension $n \times m$ and I_n be the unity matrix of dimension $n \times n$, whose subscript will be neglected if the dimension can be inferred from the context. Also, $\mathrm{diag}(x) \in \mathbb{R}^{n\times n}$ is a diagonal matrix with the ith diagonal element being x_i, while $\mathrm{diag}\{f_i(x_i)\}_{x_i\in X}$ is a diagonal matrix whose diagonal element is $f_i(x_i)$, where x_i belongs to the set X. For a symmetric matrix P, $P \geq 0$ and $P > 0$ mean P is a semipositive and positive definite matrix, respectively.

2. System model, synchronization definition, and problem formulation.

Consider a power system consisting of q conventional generators, n_r distributed energy sources, and n_l load buses. The augmented network thus has $n = n_r + n_l + q$ buses. Without loss of generality, number buses $1, \ldots, n-q$ as buses for distributed energy sources and loads, buses $n-q+1, \ldots, n$ for generator buses. Associated with each bus is a voltage phasor $V_i\angle\theta_i$, where $V_i > 0$ is the voltage magnitude and θ_i is the voltage angle of the bus. A common assumption adopted here is the voltage at each bus has been regulated to be a constant. The electric power delivered by bus i is

$$p_{e,i} = \sum_{j=1}^{n} |V_i||V_j|\bar{G}_{ij}\cos(\theta_i - \theta_j) + |V_i||V_j|\bar{B}_{ij}\sin(\theta_i - \theta_j),$$

where $\bar{B}_{ij}$ and $\bar{G}_{ij}$ are the corresponding susceptance and conductance components of the admittance matrix, respectively. Note that $\bar{G}_{ii} > 0$, $\bar{B}_{ii} < 0$ and $\bar{G}_{ij} < 0$, $\bar{B}_{ij} > 0$ if bus i and j are connected, otherwise $\bar{G}_{ij} = \bar{B}_{ij} = 0$. The rotor dynamics of generators are modeled by the swing equation

$$m_i\ddot{\theta}_i + d_i\dot{\theta}_i = p_i - p_{e,i},\ i = n-q+1, \ldots, n, \tag{1}$$

where θ_i is the generator rotor angle, $p_i > 0$ is the mechanical power input, $m_i > 0$ and $d_i > 0$ are inertia and damping coefficients, respectively.

The model for loads and energy sources can be uniformly modeled as the first dynamics

$$d_i\dot{\theta}_i = p_i - p_{e,i},\ i = 1, \dots, n-q, \tag{2}$$

where p_i and $d_i > 0$ are constants representing different physical quantities for different types of buses. First, we adopt the frequency-dependent load model [4] for which (2) represents the power balance between load demand $-p_i + d_i\dot{\theta}_i$ and injected power $p_{e,i}$. Note that $-p_i > 0$ is the power consumption independent of frequency but might be time varying, while $d_i\dot{\theta}_i$ is the frequency-dependent term. Since energy sources are usually interfaced to grids via power electronic devices such as inverters, their dynamics are mainly determined by the control logic implemented in these devices. Either implementing droop control [1] or performing maximum power point tracking (MPPT) [15], the characteristics of energy sources equipped with inverters can be captured by (2) that depicts the power balance between energy consumption induced by internal load, power supplied by energy sources, and power delivered to grids. In particular, for energy sources implementing droop control, d_i and p_i reflect the parameter and the setpoint for the droop control, respectively [1], while for energy sources implementing MPPT control, p_i is the maximum power output that could vary with weather condition for renewable energy and d_i is related to the internal frequency-dependent load. Let $(1, \dots, q_l)$ be the index set for load buses, $(q_l + 1, \dots, q_d)$ and $(q_d + 1, \dots, n - q)$ for energy source buses implementing droop control and MPPT, respectively.

Remark 2.1. For the normal operation of power systems, the load demand and power generated by renewable energy are predicted ahead so that the other dispatchable power generation can be scheduled to match the demand and meet economic requirements. In this case, the mechanical power input at conventional power generators p_i, $i = n - q + 1, \dots, n$, and setpoints for energy sources $p_i, i = q_l + 1, \dots, q_d$, implementing droop control are scheduled ahead and hence are constant. However, the power output $p_i, i = q_d + 1, \dots, n - q$, by renewable energy sources performing MPPT is usually fluctuating around the predicted value, and may exhibit sudden change when unpredictable weather condition occurs. Also, the real-time load consumption $p_i, i = 1, \dots, q_l$, does not necessarily match the predication either, especially when modern demand-side activities become more complicated. The aforementioned mismatch between real-time power generation, consumption, and their predicted values are called (real-time) disturbances in this paper, which will be explicitly expressed in the next section. □

In this paper, we use a weighted undirected graph $\mathcal{G} = (\mathcal{V}, \mathcal{E})$ to facilitate the representation of power networks. The set of nodes is $\mathcal{V} = \{1, \dots, n\}$ representing buses and undirected edges $\mathcal{E} \subseteq \mathcal{V} \times \mathcal{V}$ representing transmission lines. An undirected edge of $\mathcal{E}$ from node i to node j is denote by (i, j), meaning that buses $\mathcal{V}_i$ and $\mathcal{V}_j$ are connected by a transmission line. Denote by $\mathcal{E}_k$ the kth edge in $\mathcal{E}$ where $k \in \{1, \dots, |\mathcal{E}|\}$. When the orientation of each edge is arbitrarily assigned, the oriented incidence matrix $B \in \mathbb{R}^{n\times|\mathcal{E}|}$ is defined as $B_{ik} = 1$ if node i is the sink node of edge $\mathcal{E}_k$ and $B_{ik} = -1$ if it is the source node. Assign each edge (i, j) the weight $a_{ij} > 0$ and the weighted Laplacian is denoted by $\mathcal{L} = [l_{ij}] \in \mathbb{R}^{n\times n}$, where $l_{ii} = \sum_{j=1}^{n} a_{ij}$ and $l_{ij} = -a_{ij}$ if $i \neq j$. As a result, $\mathcal{L} = BA_vB^{\mathrm{T}}$, where $A_v = \mathrm{diag}\{a_{ij}\}_{(i,j)\in\mathcal{E}}$ is a diagonal matrix with diagonal elements being edge weights a_{ij}. Let $\lambda_i \in \mathbb{R}$, $i = 1, \dots, n$, be ordered eigenvalues of $\mathcal{L}$ such that $0 = \lambda_1 \leq \lambda_2 \leq \cdots \leq \lambda_n$. We call $\mathcal{G}_c$ the complete graph induced by $\mathcal{G}$ if $\mathcal{G}_c = (\mathcal{V}, \mathcal{E}_c)$ is an undirected complete graph with the same set of nodes as $\mathcal{G}$, for which B_c is the incidence matrix.

In this paper, we will mainly focus on power systems with zero transfer conductance $\bar{G}_{ij} = 0$ and develop the analysis framework with more concise notation. The framework can also be extended to handle the nonzero transfer conductance case (as was done in [14]) but will not be discussed here due to page limitation. Let $a_{ij} = |V_i||V_j|\bar{B}_{ij}$ be the maximal power transferred across transmission line (i,j). Let $\xi_1 = \mathrm{col}(\theta_1, \ldots, \theta_{n-q}) \in \mathbb{R}^{n-q}$ be angle vectors for buses of distributed energy sources and loads, $\xi_2 = \mathrm{col}(\theta_{n-q+1}, \ldots, \theta_n) \in \mathbb{R}^q$ for conventional generator buses and $\xi = \mathrm{col}(\xi_1, \xi_2)$ for the whole system. Denote the power profile vector $p_f = \mathrm{col}(p_1, \ldots, p_n) \in \mathbb{R}^n$, as it represents load demand and power generation in the system. Define inertia matrices $M_2 = \mathrm{diag}(\mathrm{col}(m_{n-q+1}, \ldots, m_n))$, damping matrices $D_2 = \mathrm{diag}(\mathrm{col}(d_{n-q+1}, \ldots, d_n))$ and coefficient matrix $D_1 = \mathrm{diag}(\mathrm{col}(d_1, \ldots, d_{n-q}))$. Then, following steps made in [4], the dynamics of power systems (1) and (2) can be put in vector form

$$\dot{\xi}_1 = -D_1^{-1} T_1^{\mathrm{T}} \left(B A_v \sin(B^{\mathrm{T}} \xi) - p_f \right), \tag{3}$$

$$\ddot{\xi}_2 = -M_2^{-1} D_2 \dot{\xi}_2 - M_2^{-1} T_2^{\mathrm{T}} \left(B A_v \sin(B^{\mathrm{T}} \xi) - p_f \right), \tag{4}$$

where T_1 and T_2 are matrices defined as

$$T_1^{\mathrm{T}} = \begin{bmatrix} I_{n-q} & O_{(n-q)\times q} \end{bmatrix} \in \mathbb{R}^{(n-q)\times n},\ T_2^{\mathrm{T}} = \begin{bmatrix} O_{q\times(n-q)} & I_q \end{bmatrix} \in \mathbb{R}^{q\times n}.$$

Motivated by the synchronization of coupled phase oscillators, the concept of phase cohesiveness was introduced in [13, 14]. To be self-contained here, we revisit some notations in [13, 14]. The torus is the set $\mathbb{T}^1 = [0, 2\pi]$, where 0 and 2π are associated with each other. An angle is a point $\theta \in \mathbb{T}^1$ and an arc is a connected subset of $\mathbb{T}^1$. The n-torus is the Cartesian product $\mathbb{T}^n = \mathbb{S}^1 \times \cdots \times \mathbb{S}^1$. Let $\varUpsilon_c(\xi, \gamma) \in \mathbb{T}^n$ be the closed set of angle vector $\xi = \mathrm{col}(\theta_1, \ldots, \theta_n)$ with the property that $\max_{i,j\in\{1,\ldots,n\}} |\theta_i - \theta_j| \leq \gamma$. In fact, $\varUpsilon_c(\xi, \gamma)$ is the set of angles $(\theta_1, \ldots, \theta_n)$ with the property that there exists an arc of length γ containing all $(\theta_1, \ldots, \theta_n)$ in its interior. We adapt the definition in [13, 14] to the definition of phase cohesiveness and frequency boundedness as follows.

Definition 2.2 (synchronization: phase cohesiveness and frequency boundedness). *A solution $\xi(t) : \mathbb{R}^+ \to \mathbb{T}^n$ is then said to be phase cohesive if there exists a $\gamma \in [0, \pi)$ such that $\xi(t) \in \varUpsilon_c(\xi, \gamma)$. A solution $\dot{\xi}_2(t) : \mathbb{R}^+ \to \mathbb{R}^q$ is then said to be frequency bounded if there exists an ϖ_o such that $\|\dot{\xi}_2(t)\|_\infty \leq \varpi_o$.*

The phase cohesiveness in Definition 2.2 is the same as that introduced in [13, 14] where if p_i is constant, frequency synchronization $\lim_{t\to\infty} \dot{\theta}_i - \dot{\theta}_j = 0$ can be achieved. As will be shown later, the frequency boundedness in Definition 2.2, however, relaxes frequency synchronization and enables us to study stability under time-varying disturbances caused by fluctuations in power generation and load consumption. The *objective* of this paper is to investigate the synchronization condition in the sense of Definition 2.2 under external disturbances (see Remark 2.1 and section 3 for the discussion of external disturbances).

3. Problem conversion.

The common practice in traditional transient stability analysis is to use one of the generator buses, say bus n, as the reference bus and define the grounded coordinate $\bar{\theta}_i = \theta_i - \theta_n$. In this section, we will not use the grounded coordinate to avoid eliminating one bus and losing the original network topology. Instead, we define a coordinate transformation with respect to the solution of the power flow equation.

For normal operation of power systems, the load demand is predicted ahead and the power generation is scheduled to match the demand. The match between the load demand and generation is described by the power flow equation

$$BA_v \sin(B^{\mathrm{T}}\xi) = p_f. \tag{5}$$

Equation (5) typically has numerous solutions due to its nonlinearity and the periodicity of the sine function. Solutions satisfying (5) can be represented as

$$\xi = \xi_e := \xi_o + ce_n, \tag{6}$$

where $c \in \mathbb{R}$ is an arbitrary constant and $\xi_o = \mathrm{col}(\theta_1^o, \dots, \theta_n^o) \in \mathbb{R}^n$ is some constant vector satisfying $B^{\mathrm{T}}\xi_o \neq 0$ if $p_f \neq 0$. With this notation, ξ_o captures the relative angle differences among buses, while c characterizes a uniform offset on every bus. Since c does not affect the power flow equation (5), the uniqueness of the solution is fully captured by ξ_o. In what follows, we simply call ξ_o the equilibrium point of the power system when no confusion is caused. For the operation of power systems, equilibrium point ξ_o is rescheduled by the dispatch process, when required, to match the power generation and the power demand that is predicted over time to time. Transient stability considers the time duration between two dispatch processes, and hence the equilibrium point ξ_o is assumed to be constant. Let $p_o = \mathrm{col}(p_1^o, \dots, p_n^o)$ be the dispatched power profile that describes predicted demand and scheduled power generation satisfying

$$BA_v \sin(B^{\mathrm{T}}\xi_o) = p_o. \tag{7}$$

In fact, the real-time power profile p_f does not necessarily coincide with p_o. The difference $p = p_f - p_o$ can be regarded as the disturbance to power systems under the nominal operation.

Let $\bar{\theta}_i = \theta_i - \theta_i^o,\ i = 1, \dots, n$, be the angle deviation from the equilibrium point θ_i^o. Define $\vartheta_1 = \mathrm{col}(\bar{\theta}_1, \dots, \bar{\theta}_{n-q}) \in \mathbb{R}^{n-q}$, $\vartheta_2 = \mathrm{col}(\bar{\theta}_{n-q+1}, \dots, \bar{\theta}_n) \in \mathbb{R}^q$, and $\vartheta = \mathrm{col}(\vartheta_1, \vartheta_2)$. Then, the power system composed of (3) and (4) can be rewritten as

$$\dot{\vartheta}_1 = -D_1^{-1}T_1^{\mathrm{T}}\left(BA_v\left(\sin(B^{\mathrm{T}}(\vartheta + \xi_o)) - \sin(B^{\mathrm{T}}\xi_o)\right) - p\right), \tag{8}$$

$$\ddot{\vartheta}_2 = -M_2^{-1}D_2\dot{\vartheta}_2 - M_2^{-1}T_2^{\mathrm{T}}\left(BA_v\left(\sin(B^{\mathrm{T}}(\vartheta + \xi_o)) - \sin(B^{\mathrm{T}}\xi_o)\right) - p\right), \tag{9}$$

by noting $B^{\mathrm{T}}e_n = 0$, where $\mathrm{col}(\vartheta, \dot{\vartheta}_2)$ is the state of the system.

It is observed that the equilibrium subspace for the system (8) and (9) is

$$\mathbb{E} := \{\mathrm{col}(\vartheta, \dot{\vartheta}_2) \in \mathbb{R}^n \times \mathbb{R}^q \mid \dot{\vartheta}_2 = 0_q, \vartheta = ce_n, \forall c \in \mathbb{R}\} \tag{10}$$

on which angle deviations are synchronized, i.e., $\bar{\theta}_i - \bar{\theta}_j = 0 \ \ \forall i, j = \{1, \dots, n\}$, and the frequency settles at zero. As a result, the stability with respect to an equilibrium point ξ_o is converted into the stability with respect to this equilibrium subspace $\mathbb{E}$. In essence, the dynamical systems (8) and (9) describe how power disturbances drive angles to deviate from the equilibrium subspace.

Define

$$\vartheta_c = B_c^{\mathrm{T}}\vartheta, \tag{11}$$

where B_c is the incidence matrix of induced complete graph $\mathcal{G}_c$. As a result, elements in ϑ_c are $\bar{\theta}_i - \bar{\theta}_j$ for $i \neq j\ \forall i, j \in \{1, \dots, n\}$, which are angle differences between any arbitrary two buses. Since $|\theta_i^o - \theta_j^o| \leq c_1$ and $|\bar{\theta}_i - \bar{\theta}_j| \leq c_2$ imply $|\theta_i - \theta_j| \leq c_1 + c_2$ for $c_1 + c_2 \leq \pi$, the phase cohesiveness and frequency boundedness can also be given in terms of ϑ_c an $\dot{\vartheta}_2$ as follows with one notation defined as

$$\bar{\theta}_c = \max_{i,j \in \{1,\ldots,n\}} \{|\theta_i^o - \theta_j^o|\}. \tag{12}$$

Definition 3.1. *A solution $\vartheta(t) : \mathbb{R}^+ \to \mathbb{R}^n$ is then said to be phase cohesive if there exists a $\gamma \in [0, \pi - \bar{\theta}_c)$ such that $\|\vartheta_c(t)\|_\infty \leq \gamma$. A solution $\dot{\vartheta}_2(t) : \mathbb{R}^+ \to \mathbb{R}^q$ is then said to be frequency bounded if there exists a ϖ_o such that $\|\dot{\vartheta}_2(t)\|_\infty < \varpi_o$.*

It is worth noting that considering the cohesiveness behavior in Euclidean space $\mathbb{R}^n$ and in torus $\mathbb{T}^n$ is equivalent as far as the initial condition also satisfies cohesiveness condition. Therefore, we use the Euclidean space in Definition 3.1. Since phase cohesiveness and frequency boundedness defined in Definition 3.1 imply those in Definition 2.2, it is a weakened version of Definition 2.2. In the following, we will investigate the synchronization condition in the sense of Definition 3.1 for the system described by (8) and (9). How to extend the technique developed for the system (8) and (9) to studying the stability of the original system (3) and (4) is noted as follows.

Remark 3.2. In fact, a trivial pair (θ_o, p_o) satisfying power flow equation (7) is $(\theta_o, p_o) = (0_n, 0_n)$. Due to $(\theta_o, p_o) = (0_n, 0_n)$, one has $\text{col}(\vartheta, \dot{\vartheta}_2) = \text{col}(\xi, \dot{\xi}_2)$, $p = p_f$ and $\bar{\theta}_c = 0$ which in turn recovers $(\xi, \dot{\xi}_2)$-dynamics (3) and (4) from $(\vartheta, \dot{\vartheta}_2)$-dynamics (8) and (9). As a result, the analysis techniques to be developed for $(\vartheta, \dot{\vartheta}_2)$-dynamics can be extended for $(\xi, \dot{\xi}_2)$-dynamics in the sense of Definition 2.2 by taking $(\theta_o, p_o) = (0_n, 0_n)$ without difficulty. □

4. A stability lemma.

In order to investigate the synchronization condition in the sense of Definition 3.1, we will introduce a stability lemma in this section. Consider a nonlinear system

$$\dot{x} = f(t, x), \tag{13}$$

where $x \in \mathbb{R}^n$ is the state. The state can be decomposed as $x = \text{col}(x_1, x_2)$, where $x_1 \in \mathbb{R}^{n_1}$ and $x_2 \in \mathbb{R}^{n_2}$. Define two compact sets $B(\mu) := \{x \in \mathbb{R}^n \mid \|x\| \leq \mu\}$ and $W(r) := \{x \in \mathbb{R}^n \mid V(x) \leq r\}$, where $V(x)$ is a continuously differentiable function to be given. Define $\mathcal{T}(\gamma) := \{x \in \mathbb{R}^n \mid \|x_1\| \leq \gamma\}$ for some $\gamma \in \mathbb{R}^+$. Let us assume the origin is the equilibrium point of the system (13). The first lemma is given as follows.

Lemma 4.1. *Suppose $V(x) : \mathcal{T}(\gamma) \to \mathbb{R}^+$ is a continuously differentiable function satisfying*

$$\alpha_1(\|x\|) \leq V(x) \leq \alpha_2(\|x\|), \tag{14}$$

where α_1 and α_2 are class $\mathcal{K}$ functions. Suppose the time derivative of $V(x)$ along the trajectory of the system (13) satisfies

$$\frac{\partial V}{\partial x} f(t, x) < 0 \ \forall x \notin B(\mu) \tag{15}$$

for some μ, $\gamma \in \mathbb{R}^+$.

(a) *If there exists a class $\mathcal{K}$ function α_3 such that $\alpha_3(\gamma) \geq \alpha_2(\mu)$ and $\alpha_3(\|x_1\|) \leq V(x)$ hold for $x \in \mathcal{T}(\gamma)$, then there exists a $\chi \in \mathbb{R}$ satisfying $\alpha_2(\mu) \leq \chi \leq \alpha_3(\gamma)$ such that $W(\chi)$ is an invariant set. Moreover, any trajectories starting with $x(t_o) \in W(\chi)$ are ultimately contained in $W(\alpha_2(\mu))$, i.e., there exists*

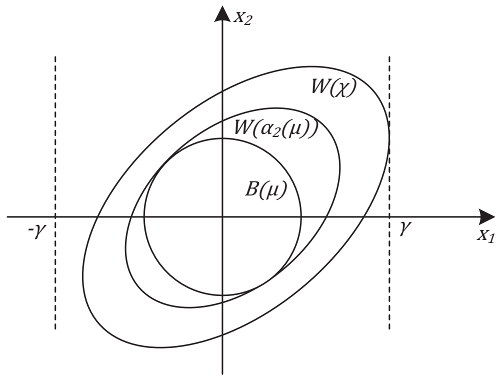

FIG. 1. *Geometric representation for sets* $B(\mu)$, $W(\alpha_2(\mu))$, $W(\chi)$, *and lines* $x_1 = \pm\gamma$.

a $T(t_o)$ *such that* $x(t) \in W(\alpha_2(\mu))$ *for* $t > T(t_o)$ *and along the trajectory* $\|x_1(t_o)\| \leq \gamma$ *for* $t > t_o$.

(b) *If there exists a class* $\mathcal{K}$ *function* α_4 *such that* $\alpha_4(\|x_2\|) \leq V(x)$ *holds for* $x \in \mathcal{T}(\gamma)$, *then* $\|x_2(t)\| \leq \varpi_o$ *for* $t > t_o$ *and some constant* ϖ_o.

Remark 4.2. The condition of this lemma is similar to that of Theorem 4.18 in [23] which concludes bounded-input–bounded-state stability for nonlinear systems. The difference is that it is additionally required in this paper that the norm of the partial state x_1 be bounded by some constant γ for the Lyapunov function to be well defined, which makes the analysis more involved. □

Proof. First, let us assume $\|x_1\| < \gamma$ such that the function $V(x)$ is well defined and defer its proof. Due to (15), the function $V(x)$ decreases outside the ball $B(\mu)$. First, we can see that $x \in B(\mu)$ implies $x \in W(\alpha_2(\mu))$, since $\|x\| \leq \mu \Rightarrow V \leq \alpha_2(\mu)$. Also, $B(\mu)$ is contained in $W(\chi)$, which follows from $x \in B(\mu) \Rightarrow x \in W(\alpha_2(\mu)) \Rightarrow x \in W(\chi)$ due to $\chi \geq \alpha_2(\mu)$. Therefore, one has $\dot{V} < 0$ at the boundary of $W(\chi)$ and hence $W(\chi)$ is an invariant set for any $\chi \geq \alpha_2(\mu)$. Moreover, any trajectories starting with $x \in W(\chi)$ will converge to and stay in $W(\alpha_2(\mu))$, because $\dot{V} < 0$ outside of the boundary of $B(\mu)$ and $W(\alpha_2(\mu))$. The relations between $B(\mu)$, $W(\alpha_2(\mu))$, and $W(\chi)$ are illustrated in Figure 1. The above argument is based on the assumption $\|x_1\| \leq \gamma$. What remains is to show the condition $\|x_1(t)\| \leq \gamma$ holds for $t \geq t_o$. As illustrated in Figure 1, this is to find the largest χ such that $\|x_1\| \leq \gamma$ is satisfied within the set $W(\chi)$. If $\chi \leq \alpha_3(\gamma)$, then $\|x_1(t)\| \leq \gamma$ for $t > t_o$ due to

$$\alpha_3(\|x_1(t)\|) \leq V(x(t)) \leq \chi. \tag{16}$$

Hence, $\alpha_2(\mu) \leq \chi \leq \alpha_3(\gamma)$ guarantees the invariant set $W(\chi)$ within which $\|x_1(t)\| \leq \gamma$ can be found. Moreover, for any trajectory starting with $x(t_o) \in W(\chi)$, it will be eventually contained in $W(\alpha_2(\mu))$ and along the trajectory $\|x_1(t)\| \leq \gamma$ holds due to (16).

Additionally, if there exists a class $\mathcal{K}$ function α_4 such that $\alpha_4(\|x_2\|) \leq V(x)$, one has

$$\alpha_4(\|x_2(t)\|) \leq V(x(t)) \leq \chi \tag{17}$$

for $t > t_o$. Let $\varpi_o \geq \alpha_4^{-1}(\chi)$, one has $\|x_2(t)\| \leq \varpi_o$. □

When class $\mathcal{K}$ functions α_1, α_3, α_3, and α_4 in Lemma 4.1 are replaced by some quadratic functions, the following corollary is obtained.

COROLLARY 4.3. *Suppose* $V(x) : \mathcal{T}(\gamma) \to \mathbb{R}^+$ *is a continuously differentiable function satisfying*

$$\alpha_1\|x\|^2 \leq V(x) \leq \alpha_2\|x\|^2,$$

where α_1 *and* α_2 *are some positive constants. Also suppose the derivative of* $V(x)$ *along the trajectory of the system (13) satisfies* $\frac{\partial V}{\partial x} f(t,x) < 0 \ \forall x \notin B(\mu)$.

(a) *If there exists a positive constant* α_3 *such that* $\gamma \geq \mu\sqrt{\alpha_2/\alpha_3}$ *and* $\alpha_3\|x_1\|^2 \leq V(x)$ *hold for* $x \in \mathcal{T}(\gamma)$, *then there exists a* $\chi \in \mathbb{R}$ *satisfying* $\alpha_2\mu^2 \leq \chi \leq \alpha_3\gamma^2$ *such that* $W(\chi)$ *is an invariant set. Moreover, any trajectories starting with* $x(t_o) \in W(\chi)$ *are ultimately contained in* $W(\alpha_2\mu^2)$ *and along the trajectory* $\|x_1(t)\| \leq \gamma$ *holds.*

(b) *If there exists a positive constant* α_4 *such that* $\alpha_4\|x_2\|^2 \leq V(x)$ *holds for* $x \in \mathcal{T}(\gamma)$, *then* $\|x_2(t)\| \leq \varpi_o$ *for* $t > t_o$ *and some* $\varpi_o > 0$.

Remark 4.4. When we set $x_1 = \vartheta_c$ and $x_2 = \dot{\vartheta}_2$, the properties (a) and (b) in Corollary 4.3 correspond to the phase cohesiveness and frequency boundedness in Definition 3.1, by noting $\|x_1\|_\infty \leq \|x_1\|$. Thus, Lemma 4.1 and Corollary 4.3 will be employed to derive the synchronization condition in the next section. □

5. Synchronization analysis.

Now, we are ready to investigate the synchronization property in the sense of Definition 3.1. First, we need to construct a class of parameterized energy functions.

5.1. Energy functions.

In [4, 18, 19], the energy function method relies on a class of energy functions derived for power systems in grounded coordinates using the multivariable Popov criterion. In this section, we will obtain a class of energy functions in the coordinate defined in section 3. The power system composed of (8) and (9) with zero disturbance $p = 0_n$ can be rewritten as

$$\dot{x} = Fx - G\psi(H^{\mathrm{T}}x) \tag{18}$$

with $x = \mathrm{col}(\vartheta, \dot{\vartheta}_2)$, where

$$\psi(H^{\mathrm{T}}x) = BA_v\left(\sin(B^{\mathrm{T}}(\vartheta + \xi_o)) - \sin(B^{\mathrm{T}}\xi_o)\right) \tag{19}$$

and

$$F = \begin{bmatrix} O_{n\times n} & T_2 \\ O_{q\times n} & -M_2^{-1}D_2 \end{bmatrix},\ G = \begin{bmatrix} T_1D_1^{-1}T_1^{\mathrm{T}} \\ M_2^{-1}T_2^{\mathrm{T}} \end{bmatrix},\ H = \begin{bmatrix} I_{n\times n} \\ O_{q\times n} \end{bmatrix}. \tag{20}$$

Note that (18) is similar to the Lur'e form, but the linear part (F, G, H) of the system is not a minimal realization due to the underactuation property of the system, namely, $e_n^{\mathrm{T}}\psi(H^{\mathrm{T}}x) = 0$. However, we will show it is still possible to find a typical energy function in the form

$$V(\vartheta, \dot{\vartheta}_2) = V_1(\vartheta, \dot{\vartheta}_2) + V_2(\vartheta), \tag{21}$$

where

$$V_1(\vartheta, \dot{\vartheta}_2) = \frac{1}{2}\begin{bmatrix} \vartheta \\ \dot{\vartheta}_2 \end{bmatrix}^{\mathrm{T}} P \begin{bmatrix} \vartheta \\ \dot{\vartheta}_2 \end{bmatrix}, \tag{22}$$

$$V_2(\vartheta) = \frac{1}{2}\beta\sum_{i=1}^{n}\sum_{j=1}^{n} a_{ij}\int_0^{\bar{\theta}_i - \bar{\theta}_j}\left[\sin(u + \theta_i^o - \theta_j^o) - \sin(\theta_i^o - \theta_j^o)\right]du \tag{23}$$

with $P \in \mathbb{R}^{(n+p)\times(n+p)}$ and $\beta \in \mathbb{R}$ to be determined. For physical systems, $V_2(\vartheta)$ can be explained as the sum of potential energy induced by conservative coupling forces across transmission lines, while depending on the choice of P, $V_1(\vartheta, \dot{\vartheta}_2)$ can be the sum of the kinetic energy and cross terms to the related energy.

The following proposition is inspired by the work [2, 19] and will be used to choose P and β later.

PROPOSITION 5.1. *Consider the dynamic system* (18) *or, equivalently, the system composed of* (8) *and* (9) *with* $p = 0_n$*. If there exist a symmetric matrix* P *and matrices* L, W, *and* X *of proper dimensions such that the following equalities are satisfied*

$$\begin{aligned} PF + F^{\mathrm{T}}P &= -LL^{\mathrm{T}}, \\ PG &= \alpha H + \beta F^{\mathrm{T}}H - LW + Xe_n^{\mathrm{T}}, \\ W^{\mathrm{T}}W &= \beta(H^{\mathrm{T}}G + G^{\mathrm{T}}H), \end{aligned} \tag{24}$$

then the energy function V *in* (21) *satisfies* $\dot{V} \le 0$ *for* $|\bar{\theta}_i - \bar{\theta}_j| < \pi - 2\bar{\theta}_c$ $\forall (i,j) \in \mathcal{E}$, *where* $\bar{\theta}_c$ *is defined in* (12).

Proof. It is straightforward to calculate $\dot{V}$ as follows:

$$\begin{aligned} \dot{V} &= \frac{1}{2}x^{\mathrm{T}}(PF + F^{\mathrm{T}}P)x - x^{\mathrm{T}}PG\psi(H^{\mathrm{T}}x) + \beta\psi^{\mathrm{T}}(H^{\mathrm{T}}x)H^{\mathrm{T}}\left[Fx - G\psi(H^{\mathrm{T}}x)\right] \\ &= -\frac{1}{2}x^{\mathrm{T}}LL^{\mathrm{T}}x - x^{\mathrm{T}}(\alpha H - LW)\psi(H^{\mathrm{T}}x) - \beta\psi^{\mathrm{T}}(H^{\mathrm{T}}x)H^{\mathrm{T}}G\psi(H^{\mathrm{T}}x) \\ &= -\frac{1}{2}x^{\mathrm{T}}LL^{\mathrm{T}}x + x^{\mathrm{T}}LW\psi(H^{\mathrm{T}}x) - \frac{1}{2}\psi^{\mathrm{T}}(H^{\mathrm{T}}x)W^{\mathrm{T}}W\psi(H^{\mathrm{T}}x) - \alpha x^{\mathrm{T}}H\psi(H^{\mathrm{T}}x) \\ &= -\frac{1}{2}\left[L^{\mathrm{T}}x + W\psi(H^{\mathrm{T}}x)\right]^{\mathrm{T}}\left[L^{\mathrm{T}}x + W\psi(H^{\mathrm{T}}x)\right] - \alpha x^{\mathrm{T}}H\psi(H^{\mathrm{T}}x) \\ &\le -\alpha x^{\mathrm{T}}H\psi(H^{\mathrm{T}}x), \end{aligned} \tag{25}$$

where we use (24) and the fact $e_n^{\mathrm{T}}\psi(H^{\mathrm{T}}x) = 0$. Note that

$$x^{\mathrm{T}}H\psi(H^{\mathrm{T}}x) = \frac{1}{2}\sum_{i=1}^{n}\sum_{j=1}^{n} a_{ij}\left(\sin(\bar{\theta}_i - \bar{\theta}_j + \theta_i^o - \theta_j^o) - \sin(\theta_i^o - \theta_j^o)\right)\left(\bar{\theta}_i - \bar{\theta}_j\right).$$

If $|\bar{\theta}_i - \bar{\theta}_j| < \pi - 2\bar{\theta}_c$ $\forall (i,j) \in \mathcal{E}$, the following holds:

$$\left[\sin(\bar{\theta}_i - \bar{\theta}_j + \theta_i^o - \theta_j^o) - \sin(\theta_i^o - \theta_j^o)\right]\left(\bar{\theta}_i - \bar{\theta}_j\right) \ge 0 \ \forall (i,j) \in \mathcal{E}.$$

Thus, $x^{\mathrm{T}}H\psi(H^{\mathrm{T}}x) \ge 0$ and $\dot{V} \le 0$. ◻

For a system of Lur'e type (18), if (F, G, H) is a minimal realization of the linear part $G_L(s)$ of the system and $Z(s) = (\alpha + \beta s)G_L(s)$ is positive real, it is guaranteed that there always exist matrices P, L, and W satisfying (24) [2] with $X = 0$. The power system in the grounded coordinates is a minimal realization of the linear part of the Lur'e system and ensures the existence of Lur'e–Postnikov-type Lyapunov function. Although the angle deviation dynamics composed of (8) and (9) is not a minimal realization, it will be shown that matrices P, L, W, and X satisfying (24) can be found.

PROPOSITION 5.2. *Let*

$$\begin{aligned} P &= \alpha\begin{bmatrix} (D - De_ne_n^{\mathrm{T}}D/d) & (D - De_ne_n^{\mathrm{T}}D/d)T_2D_2^{-1}M_2 \\ M_2D_2^{-1}T_2^{\mathrm{T}}(D - De_ne_n^{\mathrm{T}}D/d) & \beta/\alpha M_2 - M_2e_qe_q^{\mathrm{T}}M_2/d \end{bmatrix}, \\ X &= -\alpha/d\begin{bmatrix} De_n \\ M_2e_q \end{bmatrix}, \end{aligned} \tag{26}$$

where $\alpha, \beta \in \mathbb{R}$ and $d = e_n^{\mathrm{T}} D e_n$. Then, the equality (24) *is satisfied with some L and W of proper dimensions and the energy function* (21) *obtains $V = 0$ at equilibrium subspace $\mathbb{E}$.*

Proof. Following a similar derivation in [19], in order to make P, L, W, and X satisfy (24), they should be in the form of

$$P = \begin{bmatrix} P_1 & P_2^{\mathrm{T}} \\ P_2 & P_3 \end{bmatrix}, \; L = \begin{bmatrix} O & O \\ L_1 & L_2 \end{bmatrix}, \; W = \begin{bmatrix} W_1 \\ W_2 \end{bmatrix}, \; X = \begin{bmatrix} X_1 \\ X_2 \end{bmatrix}$$

and satisfy the following equalities

$$\begin{aligned} P_2^{\mathrm{T}} M_2^{-1} D_2 - P_1 T_2 &= O, \\ P_2^{\mathrm{T}} M_2^{-1} T_2^{\mathrm{T}} + P_1 T_1 D_1^{-1} T_1^{\mathrm{T}} &= \alpha I + X_1 e_n^{\mathrm{T}}, \\ P_3 M_2^{-1} D_2 + D_2 M_2^{-1} P_3 - P_2 T_2 - T_2^{\mathrm{T}} P_2^{\mathrm{T}} &= L_1 L_1^{\mathrm{T}} + L_2 L_2^{\mathrm{T}}, \\ P_2 T_1 D_1^{-1} T_1^{\mathrm{T}} + P_3 M_2^{-1} T_2^{\mathrm{T}} &= \beta T_2^{\mathrm{T}} - (L_1 W_1 + L_2 W_2) + X_2 e_n^{\mathrm{T}}, \\ W_1^{\mathrm{T}} W_1 + W_2^{\mathrm{T}} W_2 &= 2\beta T_1 D_1^{-1} T_1^{\mathrm{T}}. \end{aligned} \tag{27}$$

For simplicity, we only consider the case $LW = O$.

The first and second lines of (27) lead to

$$P_1 = \alpha D + X_1 e_n^{\mathrm{T}} D,$$

where $D = \operatorname{diag}\{D_1, D_2\}$. One should have $X_1 = \gamma D e_n$ with $\gamma \in \mathbb{R}$ to make P_1 a symmetric matrix and hence $P_1 = \alpha D + \gamma D e_n e_n^{\mathrm{T}} D$. Then, P_2 can be calculated as $P_2 = M_2 D_2^{-1} T_2^{\mathrm{T}} (\alpha D + \gamma D e_n e_n^{\mathrm{T}} D)$. The fourth line of (27) becomes

$$\begin{aligned} &\begin{bmatrix} M_2 D_2^{-1} T_2^{\mathrm{T}} (\alpha D + \gamma D e_n e_n^{\mathrm{T}} D) T_1 D_1^{-1} & P_3 M_2^{-1} \end{bmatrix} \\ &\qquad = \begin{bmatrix} O & \beta I \end{bmatrix} + \begin{bmatrix} X_2 e_{n-q}^{\mathrm{T}} & X_2 e_q^{\mathrm{T}} \end{bmatrix}. \end{aligned} \tag{28}$$

Note that

$$\alpha D + \gamma D e_n e_n^{\mathrm{T}} D = \begin{bmatrix} \alpha D_1 + \gamma D_1 e_{n-q} e_{n-q}^{\mathrm{T}} D_1 & \gamma D_1 e_{n-q} e_q^{\mathrm{T}} D_2 \\ \gamma D_2 e_q e_{n-q}^{\mathrm{T}} D_1 & \alpha D_2 + \gamma D_2 e_q e_q^{\mathrm{T}} D_2 \end{bmatrix}.$$

For (28) to hold, one should have $X_2 = \gamma M_2 e_q$ and $P_3 = \beta M_2 + \gamma M_2 e_q e_q^{\mathrm{T}} M_2$. The third line together with the fifth line of (27) becomes

$$\begin{aligned} L_1 L_1^{\mathrm{T}} + L_2 L_2^{\mathrm{T}} &= 2(\beta D_2 - \alpha M_2), \\ W_1^{\mathrm{T}} W_1 + W_2^{\mathrm{T}} W_2 &= 2\beta T_1 D_1^{-1} T_1^{\mathrm{T}}. \end{aligned} \tag{29}$$

Substituting $\dot{\xi}_2 = 0_q$ and $\xi = c_1 e_n$ into (21) leads to $V(ce_n, 0_q) = 0$ at equilibrium subspace $\mathbb{E}$ from which we obtain $\gamma = -\alpha/d$ with $d = e_n^{\mathrm{T}} D e_n$. So, P and X in (26) are obtained. Because extra freedom exists to choose L_1, L_2, W_1, and W_2 to have (29) and $LW = O$ satisfied, L and W can always be found. However, they will not be used anywhere in this paper and hence their explicit expressions are omitted here. ∎

As a result, $V(\vartheta, \dot{\vartheta}_2)$ with P given in (26) is an energy function parameterized by α and β. It is worth mentioning that the derived energy function is different from that in [18] since the additional term $X e_n^{\mathrm{T}}$ appears in (24). But it coincides with the one used in [4], when $\alpha = 0$ and $\beta = 1$. It will be shown this energy function enables us to conduct the synchronization analysis in the sense of Definition 3.1 with specific α and β.

5.2. Synchronization condition. In order to explore the synchronization condition in the sense of Definition 3.1, we use energy function (21) with P specified in (26) and set $\alpha = 1$ without loss of generality. Let $\vartheta_c = B_c^{\mathrm{T}}\vartheta \in \mathbb{R}^{n\times(n-1)/2}$ as defined in (11).

One has

$$(D - De_n e_n^{\mathrm{T}} D/d) = B_c \mathrm{diag}\{d_i d_j\} B_c^{\mathrm{T}}/d, \tag{30}$$

where $\mathrm{diag}\{d_i d_j\}$ is short for $\mathrm{diag}\{d_i d_j\}_{i,j\in\{1,\dots,n\},i\neq j}$ for the purpose of neat notation. As a result,

$$\vartheta^{\mathrm{T}}(D - De_n e_n^{\mathrm{T}} D/d)\vartheta = \vartheta_c^{\mathrm{T}} \mathrm{diag}\{d_i d_j\}\vartheta_c/d \tag{31}$$

and

$$\vartheta^{\mathrm{T}}(D - De_n e_n^{\mathrm{T}} D/d)T_2 D_2^{-1} M_2 \dot{\vartheta}_2 = \vartheta_c^{\mathrm{T}} \mathrm{diag}\{d_i d_j\} B_c^{\mathrm{T}} T_2 D_2^{-1} M_2 \dot{\vartheta}_2/d. \tag{32}$$

Hence, $V_1(\vartheta, \dot{\vartheta}_2)$ in (22) becomes

$$V_1(\vartheta, \dot{\vartheta}_2) = \frac{1}{2}\mathrm{col}(\vartheta_c, \dot{\vartheta}_2)^{\mathrm{T}} \bar{P}(\beta)\mathrm{col}(\vartheta_c, \dot{\vartheta}_2)$$

with

$$\bar{P}(\beta) = \begin{bmatrix} \mathrm{diag}\{d_i d_j\}/d & \mathrm{diag}\{d_i d_j\} B_c^{\mathrm{T}} T_2 D_2^{-1} M_2/d \\ M_2 D_2^{-1} T_2^{\mathrm{T}} B_c \mathrm{diag}\{d_i d_j\}/d & \beta M_2 - M_2 e_q e_q^{\mathrm{T}} M_2/d \end{bmatrix}. \tag{33}$$

Therefore, $V_1(\vartheta, \dot{\vartheta}_2)$ can be alternatively represented in terms of ϑ_c and $\dot{\vartheta}_2$ as does $V_2(\vartheta)$ in (23). In this subsection, we will use $V(\vartheta_c, \dot{\vartheta}_2)$, $V_1(\vartheta_c, \dot{\vartheta}_2)$, and $V_2(\vartheta_c)$ instead of $V(\vartheta, \dot{\vartheta}_2)$, $V_1(\vartheta, \dot{\vartheta}_2)$, and $V_2(\vartheta)$. A useful lemma is cited as follows.

LEMMA 5.3 (see [14]). *Let λ_2 and λ_n be the smallest and largest nonzero eigenvalues of the Laplacian matrix $\mathcal{L}$ of an undirected graph $\mathcal{G}$. For a $\vartheta \in \mathbb{R}^n$,*

$$\frac{\lambda_n}{n}\|B_c^T\vartheta\|^2 \geq \vartheta^T \mathcal{L}\vartheta \geq \frac{\lambda_2}{n}\|B_c^T\vartheta\|^2$$

holds, where B_c is the incidence matrix of the complete graph $\mathcal{G}_c$ induced by $\mathcal{G}$.

Now, we show that $V_2(\vartheta_c)$ in (23) is upper and lower bounded by nonnegative functions of ϑ_c.

LEMMA 5.4. *Let $\bar{\theta}_c$ be defined in* (12) *and $\bar{\theta}_c < \pi/2$. For a given $\gamma \in [0, \pi - 2\bar{\theta}_c)$, if $|\bar{\theta}_i - \bar{\theta}_j| \leq \gamma \ \ \forall i, j = 1, \dots, n$, then $V_2(\vartheta_c)$ satisfies*

$$\frac{1}{2n}\beta\kappa(\gamma)\lambda_2\|\vartheta_c\|_2^2 \leq V_2(\vartheta_c) \leq \frac{1}{2n}\beta\lambda_n\|\vartheta_c\|_2^2, \tag{34}$$

where

$$\kappa(\gamma) = \mathrm{sinc}(\gamma/2)\cos(\gamma/2 + \bar{\theta}_c). \tag{35}$$

Proof. For any $|u| \leq \gamma < \pi$, one has

$$\frac{\sin(u/2)}{u/2} \geq \mathrm{sinc}(\gamma/2)$$

and $\cos(u/2+x) \geq \cos(\gamma/2+\bar{\theta}_c)$ for any $|x| \leq \bar{\theta}_c$ due to $|u/2+x| < \gamma/2+\bar{\theta}_c < \pi/2$. This leads to

$$\frac{\sin(u+x)-\sin x}{u} = \frac{\cos(u/2+x)\sin(u/2)}{u/2} \geq \kappa(\gamma) \tag{36}$$

and

$$\frac{\sin(u+x)-\sin x}{u} \leq 1. \tag{37}$$

Applying (36), (37), and Lemma 5.3 yields

$$\begin{aligned} V_2(\vartheta) &= \frac{1}{2}\beta\sum_{i=1}^{n}\sum_{j=1}^{n} a_{ij}\int_0^{\bar{\theta}_i-\bar{\theta}_j} \frac{\sin(u+\theta_{ij}^o)-\sin\theta_{ij}^o}{u} u du \\ &\geq \frac{\beta}{2}\sum_{i=1}^{n}\sum_{j=1}^{n} a_{ij}\int_0^{\bar{\theta}_i-\bar{\theta}_j} \kappa(\gamma) u du = \frac{1}{2}\beta\kappa(\gamma)\vartheta^{\mathrm{T}}\mathcal{L}\vartheta \geq \frac{1}{2n}\beta\lambda_2\kappa(\gamma)\|\vartheta_c\|^2 \end{aligned}$$

and $V_2(\vartheta_c) \leq \frac{1}{2}\beta\vartheta^{\mathrm{T}}\mathcal{L}\vartheta \leq \frac{1}{2n}\beta\lambda_n\|\vartheta_c\|^2$. Thus, the proof is complete. □

The nonnegativeness of the energy function $V(\vartheta_c, \dot{\vartheta}_2)$ is guaranteed by proper selection of scalar β and demonstrated as follows.

LEMMA 5.5. *Let $\bar{\theta}_c$ be defined in* (12) *and $\bar{\theta}_c < \pi/2$. Denote the maximum inertia-damping ratio among conventional generators by $\eta = \max_{i=n-q+1,\ldots,n}(m_i/d_i)$. If $\beta > \eta$, then $V(\vartheta_c, \dot{\vartheta}_2) \geq 0$ and only obtains $V(\vartheta_c, \dot{\vartheta}_2) = 0$ at equilibrium subspace $\mathbb{E}$ in* (10). *Moreover, given a $\gamma \in [0, \pi - 2\bar{\theta}_c)$, if $|\bar{\theta}_i - \bar{\theta}_j| \leq \gamma$ $\forall i, j = 1, \ldots, n$, there exist functions $\alpha_1(\beta, \gamma)$ depending on β and γ and $\alpha_2(\beta)$ depending on β such that*

$$\alpha_1(\beta,\gamma)\|col(\vartheta_c, \dot{\vartheta}_2)\|^2 \leq V(\vartheta_c, \dot{\vartheta}_2) \leq \alpha_2(\beta)\|col(\vartheta_c, \dot{\vartheta}_2)\|^2. \tag{38}$$

Proof. To prove the nonnegativeness of $V(\vartheta_c, \dot{\vartheta}_2)$, it suffices to prove $V_1 \geq 0$, since Lemma 5.4 showed $V_2(\vartheta_c) \geq 0$. At equilibrium subspace $\mathbb{E}$, it is straightforward to see that $V_2(\vartheta_c) = 0$ and $V_1(\vartheta_c, \dot{\vartheta}_2) = 0$ due to $\vartheta_c = 0_{n\times(n-1)/2}$ and $\dot{\vartheta}_2 = 0$. We will show $\bar{P}(\beta)$ in (33) satisfies $\bar{P}(\beta) > 0$ which in turn implies $V_1(\vartheta_c, \dot{\vartheta}_2) > 0$ outside $\mathbb{E}$. According to the Schur complement, $\bar{P}(\beta) > 0$ is equivalent to

$$\beta M_2 - M_2 e_q e_q^{\mathrm{T}} M_2/d - M_2 D_2^{-1} T_2^{\mathrm{T}} B_c \mathrm{diag}\{d_i d_j\} B_c T_2 D_2^{-1} M_2/d > 0. \tag{39}$$

Note that

$$\begin{aligned} & M_2 D_2^{-1} T_2^{\mathrm{T}} B_c \mathrm{diag}\{d_i d_j\} B_c T_2 D_2^{-1} M_2/d \\ &= M_2 D_2^{-1} T_2^{\mathrm{T}} (D - D e_n e_n^{\mathrm{T}} D/d) T_2 D_2^{-1} M_2 = \begin{bmatrix} O & M_2 D_2^{-1} \end{bmatrix} \\ &\times \begin{bmatrix} (D_1 - D_1 e_{n-q} e_{n-q}^{\mathrm{T}} D_1/d) & -D_1 e_{n-q} e_q^{\mathrm{T}} D_2/d \\ -D_2 e_{n-q} e_q^{\mathrm{T}} D_1/d & (D_2 - D_2 e_q e_q^{\mathrm{T}} D_2/d) \end{bmatrix} \times \begin{bmatrix} O \\ D_2^{-1} M_2 \end{bmatrix} \\ &= M_2 D_2^{-1} M_2 - M_2 e_q e_q^{\mathrm{T}} M_2/d, \end{aligned} \tag{40}$$

where (30) is used for the first equality. As a result, (39) is implied by $\beta M_2 - M_2 D_2^{-1} M_2 > 0$ which holds for $\beta > \eta$. The nonnegativeness of $V(\vartheta_c, \dot{\vartheta}_2)$ is proved.

Note that $V_1(\vartheta, \dot{\vartheta}_2)$ can be rewritten as

$$V_1(\vartheta, \dot{\vartheta}_2) = \frac{1}{2}\mathrm{col}(\vartheta_c, \dot{\vartheta}_2)^{\mathrm{T}} \bar{P}(\eta) \mathrm{col}(\vartheta_c, \dot{\vartheta}_2) + \frac{1}{2}(\beta - \eta)\dot{\vartheta}_2^{\mathrm{T}} M_2 \dot{\vartheta}_2,$$

where $\bar{P}(\eta)$ is $\bar{P}(\beta)$ with β specified by η. Due to the aforementioned analysis, $\bar{P}(\eta) \geq 0$. Applying Lemma 5.4 gives

$$\begin{aligned} 2V &\geq \underline{\lambda}_P \|\mathrm{col}(\vartheta_c, \dot{\vartheta}_2)\|^2 + (\beta-\eta)\dot{\vartheta}_2^{\mathrm{T}} M_2 \dot{\vartheta}_2 + \beta\kappa(\gamma)\lambda_2 \|\vartheta_c\|^2/n, \\ 2V &\leq \bar{\lambda}_P \|\mathrm{col}(\vartheta_c, \dot{\vartheta}_2)\|^2 + (\beta-\eta)\dot{\vartheta}_2^{\mathrm{T}} M_2 \dot{\vartheta}_2 + \beta\lambda_n \|\vartheta_c\|^2/n, \end{aligned} \tag{41}$$

where $\underline{\lambda}_P$ and $\bar{\lambda}_P$ is the smallest and largest eigenvalue of $\bar{P}(\eta)$, respectively. Letting

$$\begin{aligned} \alpha_1(\beta,\gamma) &= \frac{1}{2}\underline{\lambda}_P + \frac{1}{2}\min\left\{\beta\kappa(\gamma)\lambda_2/n, (\beta-\eta)\underline{m}\right\}, \\ \alpha_2(\beta) &= \frac{1}{2}\bar{\lambda}_P + \frac{1}{2}\max\left\{\beta\lambda_n/n, (\beta-\eta)\bar{m}\right\}, \end{aligned} \tag{42}$$

where $\underline{m} = \min_{i=n-q+1,\dots,n}\{m_i\}$ and $\bar{m} = \max_{i=n-q+1,\dots,n}\{m_i\}$, inequality (38) is satisfied. ∎

Remark 5.6. Inequality (41) implies that $V(\vartheta_c, \dot{\vartheta}_2) \geq \alpha_3(\beta,\gamma)\|\vartheta_c\|_2$, where the function $\alpha_3(\beta,\gamma)$ can be chosen as $\alpha_3(\beta,\gamma) = \beta\kappa(\gamma)\lambda_2/(2n)$. It also implies that $V(\vartheta_c, \dot{\vartheta}_2) \geq \alpha_4(\beta)\|\dot{\vartheta}_2\|_2^2$, where $\alpha_4(\beta)$ can be chosen as $\alpha_4 = 1/2(\beta-\eta)\underline{m}$. ∎

Let us introduce some notations that will be used in the next theorem. Define the compact set $W(r) := \{\mathrm{col}(\vartheta_c, \dot{\vartheta}_2) \in \mathbb{R}^{n\times(n-1)/2+q} \mid V(\vartheta_c, \dot{\vartheta}_2) \leq r\}$ and denote the matrix

$$\Pi = \begin{bmatrix} \mathrm{diag}\{d_i d_j\} B_c^{\mathrm{T}} D^{-1}/d \\ \eta T_2^{\mathrm{T}} - M_2 e_q e_n^{\mathrm{T}}/d \end{bmatrix}. \tag{43}$$

Denote γ, β-dependent quantity

$$\iota_1(\beta,\gamma) = \min\left\{\kappa(\gamma)\lambda_2/n, (\beta-\eta)\underline{d}\right\} > 0, \tag{44}$$

where $\underline{d} = \min_{i=n-q+1,\dots,n}\{d_i\}$, $\kappa(\gamma)$ is given (35), and λ_2 is the smallest nonzero eigenvalue of Laplacian matrix $\mathcal{L}$. For convenience, we denote $\|s(t)\|_{[t_1,t_2]} = \sup_{t_1\leq t\leq t_2}\|s(t)\|$ for a bounded vector signal $s(t)$. Define disturbance-related quantities

$$\begin{aligned} \iota_2(\beta) &= \|\Pi p(t)\|_{[t_o,\infty]} + (\beta-\eta)\|T_2^{\mathrm{T}} p(t)\|_{[t_o,\infty]}, \iota_3(\beta) = \frac{\beta}{4}\|p^{\mathrm{T}}(t) T_D p(t)\|_{[t_o,\infty]}, \\ \mu(\beta,\gamma) &= \frac{\iota_2(\beta) + \sqrt{\iota_2^2(\beta) + 4\iota_1(\beta,\gamma)\iota_3(\beta)}}{2\iota_1(\beta,\gamma)}, \end{aligned} \tag{45}$$

where $T_D = T_1 D_1^{-1} T_1^{\mathrm{T}}$. Using $V(\vartheta_c, \dot{\vartheta}_2)$ as the Lyapunov function candidate, synchronization in the sense of Definition 3.1 is presented in the next theorem.

THEOREM 5.7. *Consider the system* (8) *and* (9) *with energy function* $V(\vartheta_c, \dot{\vartheta}_2)$ *in* (21). *Suppose* $\bar{\theta}_c < \pi/2$. *Let* $\gamma \in [0, \pi - 2\bar{\theta}_c)$, $\beta > \eta$, $\alpha_2(\beta)$ *be given in Lemma* 5.5, $\alpha_3(\beta,\gamma)$ *be given in Remark* 5.6, *and* $\mu(\beta,\gamma)$ *be given in* (45). *If there exist scalars* β *and* γ *such that*

$$\gamma \geq \mu(\beta,\gamma)\sqrt{\alpha_2(\beta)/\alpha_3(\beta,\gamma)} \tag{46}$$

holds, then a scalar $\chi > 0$ *satisfying* $\alpha_2(\beta)\mu^2(\beta,\gamma) \leq \chi \leq \alpha_3(\beta,\gamma)\gamma^2$ *exists such that* $W(\chi)$ *is an invariant set and synchronization in the sense of Definition* 3.1 *is achieved. In particular,*

(a) *any trajectories starting with* $col(\vartheta_c(t_o), \dot{\vartheta}_2(t_o)) \in W(\chi)$ *is ultimately contained in* $col(\vartheta_c(t), \dot{\vartheta}_2(t)) \in W(\alpha_2(\beta)\mu^2(\beta,\gamma))$ *and along the trajectory* $\|\vartheta_c(t)\|_\infty \leq \gamma$ *holds for* $t > t_o$*;*

(b) $\|\dot{\vartheta}_2(t)\|_\infty \leq \varpi_o$ *for some* ϖ_o *and* $t > t_o$*.*

If disturbance $p = 0_n$*, the trajectory will exponentially converge to the equilibrium subspace* $\mathbb{E}$*, i.e.,*

$$\lim_{t\to\infty} col(\vartheta_c(t), \dot{\vartheta}_2(t)) = col(0_{n\times(n-1)/2}, 0_q).$$

Proof. It has been shown that for $\beta > \eta$, $V(\vartheta_c, \dot{\vartheta}_2)$ is a valid energy function. The dynamical system (8) and (9) can be written as

$$\dot{x} = Fx - G\psi(H^{\mathrm{T}}x) + Gp \tag{47}$$

with F, G, H, and $\psi(\cdot)$ defined in (20) and (19), respectively. From (29), one obtains

$$LL^{\mathrm{T}} = \begin{bmatrix} O & O \\ O & L_1L_1^{\mathrm{T}} + L_2L_2^{\mathrm{T}} \end{bmatrix} = \begin{bmatrix} O & O \\ O & 2(\beta D_2 - \alpha M_2) \end{bmatrix},\ W^{\mathrm{T}}W = 2\beta T_D. \tag{48}$$

Using (24) and (26), the time derivative of $V(\vartheta_c, \dot{\vartheta}_2)$ along the trajectory of the system (47) is calculated:

$$\begin{aligned}
\dot{V} &= \frac{1}{2}x^{\mathrm{T}}(PF + F^{\mathrm{T}}P)x - x^{\mathrm{T}}PG\psi(H^{\mathrm{T}}x) + x^{\mathrm{T}}PGp \\
&\quad + \beta\psi^{\mathrm{T}}(H^{\mathrm{T}}x)H^{\mathrm{T}}\left[Fx - G\psi(H^{\mathrm{T}}x) + Gp\right] \\
&= -\frac{1}{2}x^{\mathrm{T}}LL^{\mathrm{T}}x - \frac{1}{2}\left[W\psi(H^{\mathrm{T}}x)\right]^{\mathrm{T}}\left[W\psi(H^{\mathrm{T}}x)\right] \\
&\quad - x^{\mathrm{T}}H\psi(H^{\mathrm{T}}x) - x^{\mathrm{T}}(H + \beta F^{\mathrm{T}}H + Xe_n)p + \beta\psi^{\mathrm{T}}(H^{\mathrm{T}}x)H^{\mathrm{T}}Gp \\
&= -\dot{\vartheta}_2^{\mathrm{T}}(\beta D_2 - M_2)\dot{\vartheta}_2 - \vartheta^{\mathrm{T}}s(\vartheta) - \beta s(\vartheta)^{\mathrm{T}}T_Ds(\vartheta) \\
&\quad + \beta p^{\mathrm{T}}T_Ds(\vartheta) + \vartheta^{\mathrm{T}}(I - De_ne_n^{\mathrm{T}}/d)p - \dot{\vartheta}_2^{\mathrm{T}}M_2e_qe_n^{\mathrm{T}}p/d + \beta\dot{\vartheta}_2^{\mathrm{T}}T_2^{\mathrm{T}}p,
\end{aligned}$$

where we used (48) and $s(\vartheta)$ is defined as

$$s(\vartheta) = BA_v\left(\sin(B^{\mathrm{T}}(\vartheta + \xi_o)) - \sin(B^{\mathrm{T}}\xi_o)\right).$$

A few facts are listed as follows:

$$\begin{aligned}
p^{\mathrm{T}}T_Ds(\vartheta) - s(\vartheta)^{\mathrm{T}}T_Ds(\vartheta) &\leq \frac{1}{4}p^{\mathrm{T}}T_Dp, \\
(I - De_ne_n^{\mathrm{T}}/d) &= B_c\mathrm{diag}\{d_id_j\}B_c^{\mathrm{T}}D^{-1}/d, \\
\vartheta^{\mathrm{T}}(I - De_ne_n^{\mathrm{T}}/d)p + \eta\dot{\vartheta}_2^{\mathrm{T}}T_2^{\mathrm{T}}p - \dot{\vartheta}_2^{\mathrm{T}}M_2e_qe_n^{\mathrm{T}}p/d &= [\vartheta_c^{\mathrm{T}}, \dot{\vartheta}_2^{\mathrm{T}}]\Pi p,
\end{aligned}$$

where Π is defined in (43). If $|\bar{\theta}_i - \bar{\theta}_j| \leq \gamma\ \ \forall i,j = 1,\ldots,n$, one can obtain

$$\begin{aligned}
\vartheta^{\mathrm{T}}s(\vartheta) &= \frac{1}{2}\sum_{i=1}^{n}\sum_{j=1}^{n}a_{ij}(\bar{\theta}_i - \bar{\theta}_j)\left(\sin(\bar{\theta}_i - \bar{\theta}_j + \theta_i^o - \theta_j^o) - \sin(\theta_i^o - \theta_j^o)\right) \\
&= \frac{1}{2}\sum_{i=1}^{n}\sum_{j=1}^{n}a_{ij}(\bar{\theta}_i - \bar{\theta}_j)^2\frac{\sin(\bar{\theta}_i - \bar{\theta}_j + \theta_i^o - \theta_j^o) - \sin(\theta_i^o - \theta_j^o)}{\bar{\theta}_i - \bar{\theta}_j} \\
&\geq \kappa(\gamma)(B^{\mathrm{T}}\vartheta)^{\mathrm{T}}A_v(B^{\mathrm{T}}\vartheta) \geq \kappa(\gamma)\vartheta^{\mathrm{T}}\mathcal{L}\vartheta \geq \frac{\lambda_2}{n}\kappa(\gamma)\|\vartheta_c\|^2,
\end{aligned} \tag{49}$$

where the first inequality uses (36) and for the last one we apply Lemma 5.3. Then, $\dot{V}$ is bounded as follows:

$$\dot{V} \leq -\frac{\lambda_2}{n}\kappa(\gamma)\|\vartheta_c\|^2 - \dot{\vartheta}_2^{\mathrm{T}}(\beta D_2 - M_2)\dot{\vartheta}_2 + \|\mathrm{col}(\vartheta_c, \dot{\vartheta}_2)\|\|\Pi p\|_{[t_o,\infty]} + (\beta - \eta)\|\mathrm{col}(\vartheta_c, \dot{\vartheta}_2)\|\|T_2^{\mathrm{T}} p\|_{[t_o,\infty]} + \frac{1}{4}\beta p^{\mathrm{T}} T_1 D_1^{-1} T_1^{\mathrm{T}} p.$$

As a result,

$$\dot{V} \leq -\iota_1\|\mathrm{col}(\vartheta_c, \dot{\vartheta}_2)\|^2 + \iota_2\|\mathrm{col}(\vartheta_c, \dot{\vartheta}_2)\| + \iota_3, \tag{50}$$

where ι_1, ι_2, and ι_3 are defined in (44) and (45). Thus, $\dot{V} < 0$ if

$$\|\mathrm{col}(\vartheta_c, \dot{\vartheta}_2)\| > \mu \text{ and } \|\vartheta_c\| \leq \gamma$$

for μ defined in (45), since $\|\vartheta_c\|_\infty \leq \|\vartheta_c\| \leq \gamma$. It can be easily checked that condition (1) of Corollary 4.3 is satisfied. Statements (a) and (b) follow from Corollary 4.3 and Remark 5.6 and, hence, phase cohesiveness and frequency boundedness in the sense of Definition 3.1 can be concluded. Due to (46), χ satisfying $\alpha_2(\beta)\mu^2(\beta,\gamma) \leq \chi \leq \alpha_3(\beta,\gamma)\gamma^2$ can always be found. If disturbance $p = 0_n$, $\dot{V} \leq -\iota_1\|\mathrm{col}(\vartheta_c, \dot{\vartheta}_2)\|^2$ which together with Lemma 5.5 implies the exponential convergence to the equilibrium subspace $\mathbb{E}$ locally. ∎

Remark 5.8. The difference between the classical direct method, using concepts such as closest UEP and controlling UEP (see, e.g., [8]), and the analysis in Theorem 5.7 is explained as follows. The basic principle of the direct method is to compare the energy of the postfault state and the critical energy such as defined in terms of some UEP (closest UEP or controlling UEP). If the energy at the postfault state is less than the critical energy, the energy decreases as the system trajectory evolves within the attraction basin of the stable equilibrium point (SEP). If the energy at the postfault state is greater, that means the postfault state may not lie within the attraction basin of the SEP and hence it does not necessarily converge to the corresponding SEP. These methods do not consider that the dynamical system is disturbed occasionally or persistently by disturbances even following the occurrence of the fault. However, the proof of Theorem 5.7 takes the disturbance into explicit account and studies the energy evolvement under the disturbance. If the disturbance is not too significant to invalidate the inequality (46), it is assured that there exists an invariant set $W(\chi)$ such that any trajectory starting within it will eventually be contained in the $W(\alpha_2\mu^2)$ and hence the angles stay cohesive. Instead of a pure energy comparison, this method examines stability analysis under persistent perturbation and so the analysis is more involved. More comparisons between the classic direct method and the proposed method will be provided in Remark 6.6. ∎

6. Algebraic synchronizability conditions.

In the previous section, Theorem 5.7 shows that the sufficient synchronization condition depends on the existence of the solution to the inequality (46). If so, the theorem indicates the power system is synchronizable in the sense of Definition 3.1 by choosing proper β and γ. In this section, we will discuss the existence condition of solutions to the inequality. In this sense, we call the existence condition the synchronizability condition. Also, we will fix the disturbance p, system parameters D and M_2, network topology $\mathcal{L}$ of the power system, and only focus on the variation of β and γ.

6.1. Some useful lemmas. Before we proceed, let us introduce some propositions and lemmas. Let $p, q > 0$ and $\kappa(\gamma)$ be defined in (35) and repeated as follows:

$$\kappa(\gamma) = \operatorname{sinc}(\gamma/2)\cos(\gamma/2 + \bar{\theta}_c), \tag{51}$$

where $\bar{\theta}_c$ satisfies $\bar{\theta}_c < \pi/2$. Define

$$f_l(\gamma) = \gamma^{\upsilon}\kappa^{\iota}(\gamma) \tag{52}$$

as a function of γ in the domain $\gamma \in [0, \pi - 2\bar{\theta}_c]$.

LEMMA 6.1. *$f_l(\gamma)$ is a nonnegative function having quasi-sinusoidal shape, obtains zeros at $\gamma = 0, \pi - 2\bar{\theta}_c$, and reaches its maximum at $\gamma = \gamma_o$, where $\gamma_o \leq \pi/2 - \bar{\theta}_c$ satisfying*

$$\iota\cos(\gamma_o + \bar{\theta}_c) = (\iota - \upsilon)\kappa(\gamma_o). \tag{53}$$

Proof. First, it is observed that $f_l(\gamma)$ has its zeros at $\gamma = 0, \pi - 2\bar{\theta}_c$ due to $\kappa(\pi - 2\bar{\theta}_c) = 0$. For $\gamma \in [0, \pi - 2\bar{\theta}_c]$, $\operatorname{sinc}(\gamma/2)$ and $\cos(\gamma/2 + \bar{\theta}_c)$ are monotonically decreasing functions of γ, so is $\kappa(\gamma)$ in (51) and $\kappa(\gamma) \geq 0$. Note that

$$\frac{d\kappa(\gamma)}{d\gamma} = \frac{\cos(\gamma + \bar{\theta}_c) - \kappa(\gamma)}{\gamma},$$
$$\frac{d\gamma^{\iota}\kappa^{\upsilon}(\gamma)}{d\gamma} = \gamma^{\upsilon-1}\kappa^{\iota-1}(\gamma)\left[\iota\cos(\gamma + \bar{\theta}_c) - (\iota - \upsilon)\kappa(\gamma)\right].$$

At $\gamma = 0$,

$$\iota\cos(\gamma + \bar{\theta}_c) = \iota\cos\bar{\theta}_c > (\iota - \upsilon)\kappa(\gamma) = (\iota - \upsilon)\cos\bar{\theta}_c,$$

while at $\gamma = \pi - 2\bar{\theta}_c$,

$$\iota\cos(\gamma + \bar{\theta}_c) = \iota\cos(\pi - \bar{\theta}_c) < (\iota - \upsilon)\kappa(\gamma) = 0.$$

Also, the curves $(\gamma, \iota\cos(\gamma + \bar{\theta}_c))$ and $(\gamma, (\iota - \upsilon)\kappa(\gamma))$ only intersect once at γ_o and, moreover, $\gamma_o \leq \pi/2 - \bar{\theta}_c$. We can conclude that $df_l(\gamma)/d\gamma$ is positive for $\gamma \in [0, \gamma_o)$, zero at γ_o and then negative for $\gamma \in (\gamma_o, \pi - 2\bar{\theta}_c)$. Therefore, $f_l(\gamma)$ increases with γ at $\gamma \in [0, \gamma_o)$, maximizes at γ_o, and decreases with γ at $\gamma \in (\gamma_o, \pi - 2\bar{\theta}_c]$. In summary, $f_l(\gamma)$ is a nonnegative function having quasi-sinusoidal shape. ∎

PROPOSITION 6.2. *Let $f_r(\gamma)$ be a nonincreasing $\mathcal{C}^1$ function of γ defined in the domain $\gamma \in [0, \pi - 2\bar{\theta}_c]$ satisfying $f_r(0) > 0$ and $f_r(\pi - 2\bar{\theta}_c) > 0$. Let $f_l(\gamma)$ be defined in (52). If $f_l(\gamma_o) > f_r(\gamma_o)$ for γ_o given in (53), then there exists $0 < \gamma_{\min} < \gamma_o$ and $\gamma_o < \gamma_{\max} < \pi - 2\bar{\theta}_c$ such that $f_l(\gamma_{\min}) = f_r(\gamma_{\min})$, $f_l(\gamma_{\max}) = f_r(\gamma_{\max})$, and $f_l(\gamma) > f_r(\gamma)$ for $\gamma \in (\gamma_{\min}, \gamma_{\max})$.*

Proof. By Lemma 6.1, $f_l(\gamma)$ is a quasi-sinusoidal function of γ maximized at $\gamma = \gamma_o$. If $f_l(\gamma) > f_r(\gamma)$ at $\gamma = \gamma_o$, $(\gamma, f_l(\gamma))$ must intersect with $(\gamma, f_r(\gamma))$ at least at two points, say $\gamma = \gamma_{\min}$ and $\gamma = \gamma_{\max}$ as illustrated in Figure 2, as $f_r(\gamma)$ is a nonincreasing $\mathcal{C}^1$ function. In particular, there exists a domain $\gamma \in (\gamma_{\min}, \gamma_{\max})$ within which line segments $(\gamma, f_r(\gamma))$ is above $(\gamma, f_l(\gamma))$. Then, the proof is complete. ∎

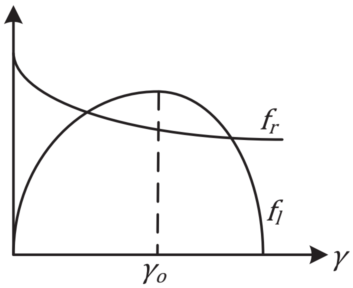

FIG. 2. *The schematic diagram for functions $f_l(\gamma)$ and $f_r(\beta)$.*

6.2. Synchronizability condition. We are ready to investigate the synchronizability condition. Inequality (46) in Theorem 5.7 is equivalent to

$$f_l(\gamma) \geq f_r(\gamma, \beta), \tag{54}$$

where

$$f_l(\gamma) := \alpha_3 \gamma^2/\rho = \gamma^2 \kappa^3(\gamma),$$
$$f_r(\gamma, \beta) := \alpha_2 \mu^2/\rho = \left(\frac{\iota_2 + \sqrt{\iota_2^2 + 4\iota_1 \iota_3}}{2\iota_1/\kappa(\gamma)} \right)^2 \frac{\alpha_2}{\alpha_3/\kappa(\gamma)} \tag{55}$$

with $\rho = \alpha_3/\kappa^3(\gamma)$. Note that α_2, ι_2, and ι_3 are functions of β, α_3, ι_1, and μ are functions of β and γ. For the purpose of neat notation, we make the dependence implicit when no confusion is caused.

By Lemma 6.1, we can check $\kappa(\gamma)$ is a monotonically decreasing function and $f_l(\gamma)$ is a quasi-sinusoidal function of γ. According to Remark 5.6, $\alpha_3 = \frac{1}{2n}\beta\kappa(\gamma)\lambda_2$ and $\alpha_3/\kappa(\gamma) = \frac{1}{2n}\beta\lambda_2$ is a constant. Observing the definition of ι_1, ι_2, and ι_3 in (44) and (45), for a fixed β, $f_r(\gamma, \beta)$ is a nonincreasing function of γ and satisfies

$$\lim_{\gamma\to 0} f_r(\gamma, \beta) > 0, \quad \lim_{\gamma\to \pi - 2\bar{\theta}_c} f_r(\gamma, \beta) > 0.$$

Then, the next lemma directly follows from Proposition 6.2.

LEMMA 6.3. *Let $f_l(r)$ and $f_r(\gamma, \beta)$ be defined in* (55)*. If $f_l(\gamma_o) > f_r(\beta, \gamma_o)$ holds for some $\beta = \beta_o$, where γ_o satisfies*

$$3\cos(\gamma_o + \bar{\theta}_c) = \kappa(\gamma_o), \tag{56}$$

then $f_l(\gamma) \geq f_r(\beta_o, \gamma)$ holds for β_o and $\gamma \in [\gamma_{\min}, \gamma_{\max}]$, where $\gamma = \gamma_{\min}, \gamma_{\max}$ are two solutions to $f_l(\gamma) = f_r(\beta_o, \gamma)$.

Lemma 6.3 leaves a question of how to select a proper β_o. One option is $\beta_{\min} = \arg\min_{\beta\in[\eta,\infty)} f_r(\gamma_o, \beta)$ which makes the inequality $f_l(\gamma_o) > f_r(\beta, \gamma_o)$ more likely to hold. However, it is not possible to explicitly calculate $\beta_{\min}$ due to the complexity of function $f_r(\gamma_o, \beta)$. In what follows, we will explicitly select a β_o as

$$\beta = \beta_o = \eta + \frac{\kappa(\gamma_o)\lambda_2}{n\underline{d}}, \tag{57}$$

where γ_o is given in (56). As a result, $\iota_1 = \lambda_2 \min\{\kappa(\gamma), \kappa(\gamma_o)\}/n$ is a nonincreasing function of γ (see definition of ι_1 in (44)). With $\beta = \beta_o$, one has

$$\frac{\alpha_2}{\alpha_3/\kappa(\gamma)} = \frac{\frac{1}{2}\bar{\lambda}_P + \frac{1}{2}\max\{\beta_o\lambda_n/n, (\beta_o - \eta)\bar{m}\}}{\frac{1}{2n}\beta_o\lambda_2} \leq \frac{n\bar{\lambda}_P}{\beta_o\lambda_2} + \frac{\max\{\lambda_n, n\bar{m}\}}{\lambda_2}.$$

Then, $\sigma(\gamma) \geq f_r(\gamma, \beta_o)$ with $\sigma(\gamma)$ defined as

$$\sigma(\gamma) = \left(\frac{\iota_2(\beta_o) + \sqrt{\iota_2^2(\beta_o) + 4\iota_3(\beta_o)\iota_1(\gamma)}}{2\iota_1(\beta_o,\gamma)/\kappa(\gamma)}\right)^2 \left(\frac{n\bar{\lambda}_P}{\beta_o\lambda_2} + \frac{\max\{\lambda_n, n\bar{m}\}}{\lambda_2}\right). \tag{58}$$

It is worth noting that ι_2 and ι_3 in (58) become constants by choosing β_o in (57). Since $\iota_1(\beta_o,\gamma)/\kappa(\gamma)$ is a nondecreasing function of γ, it is observed that $\sigma(\gamma)$ is a nonincreasing function of γ. We are ready to present the next theorem.

THEOREM 6.4. *Consider the system of* (8) *and* (9). *Let* γ_o *be given in* (56). *If*

$$\gamma_o^2\kappa^3(\gamma_o) > \sigma(\gamma_o) \tag{59}$$

with $\sigma(\gamma)$ *defined in* (58), *there exist* $\gamma_{\min}, \gamma_{\max}$ *as solutions to* $f_l(\gamma) = f_r(\beta_o, \gamma)$ *satisfying* $\gamma_{\min} < \gamma_{\max}$ *such that for any* $\gamma \in [\gamma_{\min}, \gamma_{\max}]$ *the inequality* (46) *is satisfied and the synchronization in the sense of Definition* 3.1 *can be achieved. Moreover, for* $\chi \in [\underline{\alpha}, \bar{\alpha}]$, *where* $\underline{\alpha} = \alpha_2(\beta_o)\mu(\beta_o, \gamma_{\min})^2$ *and* $\bar{\alpha} = \max_{r\in[\gamma_{\min},\gamma_{\max}]}\{\alpha_3(\beta_o,\gamma)\gamma^2\}$, *any trajectories starting within col*$(\vartheta_c, \dot{\vartheta}_2) \in W(\chi)$ *eventually converge to col*$(\vartheta_c, \dot{\vartheta}_2) \in W(\underline{\alpha})$.

Proof. Since $\sigma(\gamma_o) \geq f_r(\gamma_o, \beta_o)$, $\gamma_o^2\kappa^3(\gamma_o) > \sigma(\gamma_o)$ implies $\gamma_o^2\kappa^3(\gamma_o) > f_r(\gamma_o, \beta_o)$. Applying Lemma 6.3 shows $f_l(\gamma) \geq f_r(\beta_o, \gamma)$ holds for β_o and $\gamma \in [\gamma_{\min}, \gamma_{\max}]$, where $\gamma = \gamma_{\min}, \gamma_{\max}$ are two solutions to $f_l(\gamma) = f_r(\beta_o, \gamma)$. $f_l(\gamma) \geq f_r(\beta_o, \gamma)$ implies that the condition (46) of Theorem 5.7 is satisfied for $\beta = \beta_o$ and $\gamma \in [\gamma_{\min}, \gamma_{\max}]$ due to (55). It, in turn, shows that the synchronization in the sense of Definition 3.1 can be achieved.

Now, we focus on the "moreover" part. Let us examine the upper and lower bound for χ, that is, $\alpha_3\gamma^2$ and $\alpha_2\mu^2$ with $\beta = \beta_o$ and $\gamma \in [\gamma_{\min}, \gamma_{\max}]$. We calculate

$$\alpha_3(\beta_o,\gamma)\gamma^2 = \frac{1}{2n}\beta_o\lambda_2\kappa(\gamma)\gamma^2,$$

$$\alpha_2(\beta_o)\mu^2(\beta_o,\gamma) = \left(\frac{\iota_2(\beta_o) + \sqrt{\iota_2^2(\beta_o) + 4\iota_1(\gamma)\iota_3(\beta_o)}}{2\iota_1(\beta_o,\gamma)}\right)^2 \times \left(\frac{1}{2}\bar{\lambda}_P + \frac{1}{2}\max\{\beta_o\lambda_n/n, (\beta_o - \eta)\bar{m}\}\right).$$

Since $\iota_1(\beta_o,\gamma)$ is a nonincreasing function of γ, $\alpha_2(\beta_o)\mu^2(\beta_o,\gamma)$ is a nondecreasing function of γ. By Lemma 6.1, $\alpha_3(\beta_o,\gamma)\gamma^2$ is a function of γ having quasi-sinusoidal shape. One has

$$\underline{\alpha} = \alpha_2(\beta_o)\mu(\beta_o,\gamma_{\min})^2 \leq \alpha_2(\beta_o)\mu(\beta_o,\gamma)^2,$$
$$\alpha_3(\beta_o,\gamma)\gamma^2 \leq \bar{\alpha} = \max_{\gamma\in[\gamma_{\min},\gamma_{\max}]}\{\alpha_3(\beta_o,\gamma)\gamma^2\}.$$

Then, the maximum range for $\chi \in [\alpha_2(\beta_o)\mu(\beta_o,\gamma)^2, \alpha_3(\beta_o,\gamma)\gamma^2]$ is $[\underline{\alpha}, \bar{\alpha}]$.

For any $\chi \in [\underline{\alpha}, \bar{\alpha}]$, one can find $\gamma_1 = \arg\min_{\gamma \in [\gamma_{\min}, \gamma_{\max}]}\{\alpha_3(\beta_o, \gamma)\gamma^2 = \chi\}$. Since $\alpha_2(\beta_o)\mu^2(\beta_o, \gamma_1) < \chi \leq \alpha_3(\beta_o, \gamma_1)\gamma_1^2$, applying Theorem 5.7 shows any trajectories starting within $\mathrm{col}(\vartheta_c, \dot{\vartheta}_2) \in W(\chi)$ are ultimately contained in the invariant set $W(\alpha_2(\beta_o)\mu^2(\beta_o, \gamma_1))$. Set $\chi' = \alpha_2(\beta_o)\mu^2(\beta_o, \gamma_1) \geq \alpha_2(\beta_o)\mu^2(\beta_o, \gamma_{\min})$ and repeat the above argument with χ replaced by $\chi' < \chi$. It is noted χ' and γ_1 decrease until $\chi = \underline{\alpha}$. Then, we can prove the trajectory eventually converges to the invariant set $W(\underline{\alpha})$. ∎

First, Theorem 6.4 shows that the synchronization is closely related to the network structure of power systems. Let us examine the synchronizability condition (59). For fixed system parameters D and M_2, the left-hand side (LHS) of (59) is a constant while the value of the right-hand side (RHS) is affected by the eigenvalue of the network Laplacian $\mathcal{L}$. Specifically, if the eigenvalue λ_n is small and algebraic connectivity λ_2 is large, the RHS of (59) obtains a small value. By Theorem 6.4, power systems having such kind of network topology are more likely to be stable. Therefore, the network topology plays a very important role in the stability of power systems. Second, the synchronizability condition shows that both damping and inertia of conventional generators will play roles in synchronization compared to [14] where the role of inertia was hidden due to the singular perturbation technique. Third, the magnitude and location of the disturbance where it is injected into the systems importantly affect the synchronization by noting that the p-related term involves the structural information B_c. Hence, the condition can be potentially used to plan the location of the renewable energy, whose intermittent and stochastic fluctuation are regarded as the disturbance to the system, such that power systems could have better stability performance.

We can derive a special version of Theorems 5.7 and 6.4 in the absence of a disturbance, i.e., $p = 0$.

COROLLARY 6.5. *Consider the system of* (8) *and* (9) *with* $p = 0$. *If there exists a* β *such that the trajectory starts with* $V(\vartheta_c, \dot{\vartheta}_2) \leq \bar{\alpha}(\beta)$, *where* $V(\vartheta_c, \dot{\vartheta}_2)$ *given in* (21) *is a function of* β *and*

$$\bar{\alpha}(\beta) = \max_{r \in [0, \pi - 2\bar{\theta}_c]} \{\alpha_3(\beta, \gamma)\gamma^2\},$$

it eventually converges to equilibrium subspace $\mathbb{E}$ *defined in* (10).

Proof. The proof basically follows from that of Theorems 5.7 and 6.4. First, $p = 0$ implies $\mu(\beta, \gamma) = 0$ in (45) which in turn shows (46) is always satisfied for $\gamma \in [0, \pi - 2\bar{\theta}_c]$. Theorem 5.7 shows that any trajectories starting with $\mathrm{col}(\vartheta_c(t_o), \dot{\vartheta}_2(t_o)) \in W(\chi)$ for $\chi \in [0, \alpha_3(\beta, \gamma)\gamma^2]$ ultimately converge to equilibrium subspace $\mathbb{E}$ again due to $\mu(\beta, \gamma) = 0$. Noting that $\alpha_3(\beta, \gamma)\gamma^2 \leq \bar{\alpha}(\beta)$, the proof is thus complete. ∎

Remark 6.6. Theorem 6.4 and Corollary 6.5 can be used to assess the stability of power systems when a fault occurs. When $p \neq 0$, if the postfault energy satisfies $V(\vartheta_c, \dot{\vartheta}_2) \leq \bar{\alpha}$ in Theorem 6.4 after the fault is cleared, the system trajectory will go to the invariant set $W(\underline{\alpha})$, angles stay cohesive, and frequencies are bounded. When $p = 0$, if the postfault energy satisfies $V(\vartheta_c, \dot{\vartheta}_2) \leq \bar{\alpha}(\beta)$ for some β after the fault is cleared, the system trajectory will go to the equilibrium subspace $\mathbb{E}$.

Since the bound of the sine function was used to facilitate the analysis (see (49)), the stability results thus obtained in Theorem 6.4 and Corollary 6.5 would be more conservative than the advanced versions of classic direct methods that exploit the fault-on trajectory behavior with respect to the structural properties of equilibrium points. However, they have two advantages over the basic direct methods such as using the closest UEP. First, they are less computationally expensive, since it is not necessary to find the closest UEP which requires one to exhaust all solutions of the power flow equation and so is computationally difficult for a large-scale system. Second, the closest UEP method requires that all the equilibrium points be hyperbolic, while Theorem 6.4 and Corollary 6.5 do not impose any constraints on equilibrium points. Hence, the proposed method can be regarded as an alternative direct method. □

7. Small disturbance analysis.

Small-disturbance stability analysis is concerned with the ability of the power system to maintain synchronism under small disturbances. The disturbances are considered to be sufficiently small such that linearization of system equations is allowed to be performed. Consider deviation dynamics (8) and (9) of power systems under a small disturbance $p \approx 0$. It allows linearization around an equilibrium solution. Note that $\sin(\bar{\theta}_i - \bar{\theta}_j + \theta_{ij}^o)$ in (8) and (9) can be approximated around $\bar{\theta}_i - \bar{\theta}_j = 0$ as follows:

$$\sin(\bar{\theta}_i - \bar{\theta}_j + \theta_{ij}^o) \approx \sin\theta_{ij}^o + \cos\theta_{ij}^o(\bar{\theta}_i - \bar{\theta}_j).$$

Let $\bar{\mathcal{L}} = B\mathrm{diag}(a_{ij}\cos\theta_{ij}^o)B^{\mathrm{T}}$. The linearized dynamics of (8) and (9) is

$$\dot{\vartheta}_1 = -D_1^{-1}T_1\bar{\mathcal{L}}\vartheta, \tag{60}$$

$$\ddot{\vartheta}_2 = -M_2^{-1}D_2\dot{\vartheta}_2 - M_2^{-1}T_2\bar{\mathcal{L}}\vartheta. \tag{61}$$

We will still use the energy function (21) for the stability analysis. Since the sinusoidal coupling term is replaced by linear coupling, $V_2(\vartheta)$ in (23) becomes

$$V_2(\vartheta) = \frac{1}{2}\beta\sum_{i=1}^{n}\sum_{j=1}^{n} a_{ij}\cos\theta_{ij}^o \int_0^{\bar{\theta}_i - \bar{\theta}_j} u du.$$

Following the proof of Lemma 5.4, the bound of the energy function V in (21) is calculated as follows:

$$\alpha_1\|\mathrm{col}(\vartheta_c, \dot{\vartheta}_2)\|^2 \le V(\vartheta_c, \dot{\vartheta}_2) \le \alpha_2\|\mathrm{col}(\vartheta_c, \dot{\vartheta}_2)\|^2$$

with

$$\alpha_1(\beta) = \frac{1}{2}\underline{\lambda}_P + \frac{1}{2}\min\left\{\beta\bar{\lambda}_2/n, (\beta-\eta)\underline{m}\right\},$$
$$\alpha_2(\beta) = \frac{1}{2}\bar{\lambda}_P + \frac{1}{2}\max\left\{\beta\bar{\lambda}_n/n, (\beta-\eta)\bar{m}\right\},$$

where $\bar{\lambda}_2$ and $\bar{\lambda}_n$ are the smallest and largest nonzero eigenvalues of $\bar{\mathcal{L}}$, respectively. Moreover, the derivative of the energy function along the trajectory of the system (60) and (61) is

$$\dot{V} = -\dot{\vartheta}_2^{\mathrm{T}}(\beta D_2 - M_2)\dot{\vartheta}_2 - \Omega^{\mathrm{T}}\bar{\mathcal{L}}\Omega - \beta\vartheta^{\mathrm{T}}\bar{L}T_1D_1^{-1}T_1^{\mathrm{T}}\bar{L}\vartheta \le -\iota(\beta)\|\mathrm{col}(\vartheta_c, \dot{\vartheta}_2)\|^2,$$

where $\vartheta_c = B_c^{\mathrm{T}}\vartheta$ and $\iota(\beta) = \min\left\{\bar{\lambda}_2/n, (\beta-\eta)\underline{d}\right\}$. Using linear system theory, the local exponential convergence rate is $r = \iota(\beta)/\alpha_2(\beta)$ with β to be specified. Choosing $\beta = \beta_o := \eta + \frac{\bar{\lambda}_2}{n\underline{d}}$ yields

$$r = \frac{2}{n\bar{\lambda}_P/\bar{\lambda}_2 + \max\left\{\beta_o\bar{\lambda}_n/\bar{\lambda}_2, \bar{m}/\underline{d}\right\}}.$$

Therefore, for larger $\bar{\lambda}_2$ and smaller $\bar{\lambda}_n/\bar{\lambda}_2$ ratio, system trajectories tend to converge to the equilibrium subspace much faster.

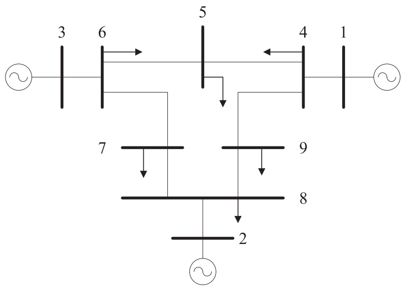

(a) IEEE 9-bus test system.

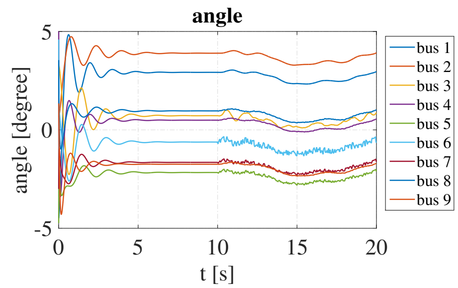

(b) Bus angles change with time.

FIG. 3. *Illustration of phase cohesiveness for the power system in difference network configurations.*

TABLE 1
Equilibrium point and nominal power profile of 9 *buses.*

Bus number	1	2	3	4	5	6	7	8	9
p_i^o (per unit)	1.17	1.63	0.85	-0.2	-0.9	-0.1	-1	-0.2	-1.25
θ_i^o(rad)	0.0888	0.1058	0.0054	0.0464	0	0.027	0.0090	0.0547	0.0073

8. Simulation. Let us consider the IEEE 9-bus test system illustrated in Figure 3(a). Buses $1, 2, 3$ are buses equipped with conventional generators while the other buses are frequency-dependent load buses. The line parameters $a_{ij} \in [10, 40]$ are randomly picked. The nominal power profile p_o is given in Table 1. Then, the SEP ξ_o can be calculated using (7) and is given in Table 1. As a result, $\bar{\theta}_c = 0.1058$ rad. The system parameter d_i is randomly generated within the range $d_i \in [0.7, 1]$ and m_i is within the range $m_i \in [0.5, 1]$. For $t \in [0, 10)$ s, since the equilibrium point is locally stable, the angles will settle to that equilibrium point. After $t = 10$ s, a random disturbance is injected at bus 6 to emulate the power consumption fluctuation. The disturbance will change its value randomly every 0.05 s, but its magnitude is bounded, i.e., $\sup_{t\in[0,\infty)} |p(t)| < 0.2$ per unit. For the synchronizability condition in Theorem 6.4, it is verified that the LHS of (59) is 0.5215 and the RHS is 0.5173 and thus (59) is satisfied. It is concluded that the angle and frequency cohesiveness can be achieved in the sense of Definition 3.1. Figure 3(b) illustrates the simulation result, which shows that angles stay cohesive even when the disturbance is injected after 10 s.

9. Conclusion. In this paper, we presented the stability analysis of power systems from the synchronization perspective in terms of phase cohesiveness and frequency boundedness. We proposed a novel definition to characterize the stability under time-varying disturbances. We first introduce a coordinate transformation that converts the original system into a deviation system. Then, a parameterized Lyapunov function was derived for the deviation system, and a specific Lyapunov-based analysis method (including the stability lemma) was proposed and led to the synchronization conditions characterized by the inequality. Finally, the algebraic synchronizability condition was attained by further analyzing the synchronization inequality. The novel analysis method leads to a purely algebraic condition, showing that the stability of power systems is related to the network topology, model parameters and affected by disturbances. Finally, the numerical simulation confirms the theoretical analysis.

REFERENCES

[1] N. Ainsworth and S. Grijalva, *A structure-preserving model and sufficient condition for frequency synchronization of lossless droop inverter-based ac networks*, IEEE Trans. Power Syst., 28 (2013), pp. 4310–4319.

[2] B. Anderson, *Stability of control systems with multiple nonlinearities*, J. Franklin Inst., 282 (1966), pp. 155–160.

[3] T. Athay, R. Podmore, and S. Virmani, *A practical method for the direct analysis of transient stability*, IEEE Trans. Power Apparat. Syst., PAS-98 (1979), pp. 573–584.

[4] A. Bergen and D. Hill, *A structure preserving model for power system stability analysis*, IEEE Trans. Power Apparat. Syst., PAS-100 (1981), pp. 25–35.

[5] S. Boccaletti, V. Latora, T. Moreno, M. Chavez, and D. Hwang, *Complex networks: Structure and dynamics*, Phys. Rep., 424 (2006), pp. 175–308.

[6] J. Buck and E. Buck, *Biology of synchronous flashing of fireflies*, Nature, 211 (1966), pp. 562–564.

[7] H. Chiang and C. Chu, *Theoretical foundation of the BCU method for direct stability analysis of network-reduction power system. Models with small transfer conductances*, IEEE Trans. Circuits Syst. I, Fundam. Theory Appl., 42 (1995), pp. 252–265.

[8] H. Chiang, C. Chu, and G. Cauley, *Direct stability analysis of electric power systems using energy functions: Theory, applications, and perspective*, Proc. IEEE, 83 (1995), pp. 1497–1529.

[9] Y. Choi, S. Ha, and S. Yun, *Complete synchronization of Kuramoto oscillators with finite inertia*, Phys. D, 240 (2011), pp. 32–44.

[10] Y. Choi, Z. Li, S. Ha, X. Xue, and S. Yun, *Complete entrainment of Kuramoto oscillators with inertia on networks via gradient-like flow*, J. Differential Equations, 257 (2014), pp. 2591–2621.

[11] N. Chopra and M. Spong, *On exponential synchronization of Kuramoto oscillators*, IEEE Trans. Automat. Control, 54 (2009), pp. 353–357.

[12] S. Chung and J. Slotine, *On synchronization of coupled Hopf-Kuramoto oscillators with phase delays*, in 49th IEEE Conference on Decision and Control, IEEE, Piscataway, NJ, 2010, pp. 3181–3187.

[13] F. Dörfler and F. Bullo, *On the critical coupling for Kuramoto oscillators*, SIAM J. Appl. Dyn. Syst., 10 (2011), pp. 1070–1099.

[14] F. Dorfler and F. Bullo, *Synchronization and transient stability in power networks and nonuniform Kuramoto oscillators*, SIAM J. Control Optim., 50 (2012), pp. 1616–1642.

[15] F. Dörfler, J. W. Simpson-Porco, and F. Bullo, *Breaking the hierarchy: Distributed control and economic optimality in microgrids*, IEEE Trans. Control Netw. Syst., 3 (2016), pp. 241–253.

[16] A. El-Abiad and K. Nagappan, *Transient stability regions of multimachine power systems*, IEEE Trans. Power Apparat. Syst., PAS-85 (1966), pp. 169–179.

[17] A. Franci, A. Chaillet, and W. Pasillas-Lépine, *Phase-locking between Kuramoto oscillators: Robustness to time-varying natural frequencies*, in 49th IEEE Conference on Decision and Control, IEEE, Piscataway, NJ, 2010, pp. 1587–1592.

[18] D. Hill and C. Chong, *Lyapunov functions of Lur'e-Postnikov form for structure preserving models of power systems*, Automatica J. IFAC, 25 (1989), pp. 453–460.

[19] D. J. Hill and A. R. Bergen, *Stability analysis of multimachine power networks with linear frequency dependent loads*, IEEE Trans. Circuits Syst., 29 (1982), pp. 840–848.

[20] D. J. Hill and G. Chen, *Power systems as dynamic networks*, in IEEE International Symposium on Circuits and Systems, IEEE, Piscataway, NJ, 2006, pp. 722–725.

[21] Z. Huang, S. Jin, and R. Diao, *Predictive dynamic simulation for large-scale power systems through high-performance computing*, in High Performance Computing, Networking, Storage and Analysis (SCC), IEEE, Piscataway, NJ, 2012, pp. 347–354.

[22] A. Jadbabaie, N. Motee, and M. Barahona, *On the stability of the Kuramoto model of coupled nonlinear oscillators*, in Proceedings of American Control Conference, Vol. 5, American Automatic Control Council, Evanston, IL, 2004, pp. 4296–4301.

[23] H. Khalil, *Nonlinear Systems*, 3rd ed., Prentice Hall, Upper Saddle River, NJ, 2002.

[24] Y. Kuramoto, *Self-entrainment of a population of coupled non-linear oscillators*, in International Symposium on Mathematical Problems in Theoretical Physics, Springer, Berlin, 1975, pp. 420–422.

[25] R. H. Lasseter, *MicroGrids*, in IEEE Power Engineering Society Winter Meeting, Vol. 1, IEEE, Piscataway, NJ, 2002, pp. 305–308.

[26] X. Li and G. Chen, *Synchronization and desynchronization of complex dynamical networks: An engineering viewpoint*, IEEE Trans. Circuits Syst. I, Fundam. Theory Appl., 50 (2003), pp. 1381–1390.
[27] G. A. Lüders, *Transient stability of multimachine power systems via the direct method of Lyapunov*, IEEE Trans. Power Apparat. Syst., PAS-90 (1971), pp. 23–36.
[28] P. Monzón and F. Paganini, *Global considerations on the Kuramoto model of sinusoidally coupled oscillators*, in 44th IEEE Conference on Decision and Control and 2005 European Control Conference, IEEE, Piscataway, NJ, 2005, pp. 3923–3928.
[29] I. Nagel, L. Fabre, M. Pastre, F. Krummenacher, R. Cherkaoui, and M. Kayal, *High-speed power system transient stability simulation using highly dedicated hardware*, IEEE Trans. Power Syst., 28 (2013), pp. 4218–4227.
[30] J. W. Simpson-Porco, F. Dörfler, and F. Bullo, *Synchronization and power sharing for droop-controlled inverters in islanded microgrids*, Automatica J. IFAC, 49 (2013), pp. 2603–2611.
[31] S. Strogatz, *Exploring complex networks*, Nature, 410 (2001), pp. 268–276.
[32] H. Tanaka, A. Lichtenberg, and S. Oishi, *First order phase transition resulting from finite inertia in coupled oscillator systems*, Phys. Rev. Lett., 78 (1997), pp. 2104–2107.
[33] H. Tanaka, A. Lichtenberg, and S. Oishi, *Self-synchronization of coupled oscillators with hysteretic responses*, Phys. D, 100 (1997), pp. 279–300.
[34] M. Verwoerd and O. Mason, *On computing the critical coupling coefficient for the Kuramoto model on a complete bipartite graph*, SIAM J. Appl. Dyn. Syst., 8 (2009), pp. 417–453.
[35] X. Wang and G. Chen, *Complex networks: Small-world, scale-free and beyond*, IEEE Circuits Syst. Mag., 3 (2003), pp. 6–20.
[36] A. Winfree, *Biological rhythms and the behavior of populations of coupled oscillators*, J. Theoret. Biol., 16 (1967), pp. 15–42.
[37] C. Wu, *Synchronization in Complex Networks of Nonlinear Dynamical Systems*, World Scientific, Singapore, 2007.
[38] L. Wu and C. Chua, *Synchronization in an array of linearly coupled dynamical systems*, IEEE Trans. Circuits Syst. I, Fundam. Theory Appl., 42 (1995), pp. 430–447.
[39] L. Zhu and D. Hill, *Transient stability analysis of microgrids with network-preserving structure*, in 6th IFAC Workshop on Distributed Estimation and Control in Networked Systems, Vol. 49, Curran Associates, Red Hook, NY, 2016, pp. 339–344.